

Can optimized effective potentials be determined uniquely?

So Hirata, Stanislav Ivanov, Ireneusz Grabowski,^{a)} and Rodney J. Bartlett^{b)}
Quantum Theory Project, University of Florida, Gainesville, Florida 32611

Kieron Burke

Department of Chemistry, Rutgers University, 610 Taylor Road, Piscataway, New Jersey 08854

James D. Talman

Department of Applied Mathematics and Centre for Chemical Physics, University of Western Ontario, London, Ontario, Canada N6A 5B7

(Received 12 March 2001; accepted 2 May 2001)

Local (multiplicative) effective exchange potentials obtained from the linear-combination-of-atomic-orbital (LCAO) optimized effective potential (OEP) method are frequently unrealistic in that they tend to exhibit wrong asymptotic behavior (although formally they should have the correct asymptotic behavior) and also assume unphysical rapid oscillations around the nuclei. We give an algebraic proof that, with an infinity of orbitals, the kernel of the OEP integral equation has one and only one singularity associated with a constant and hence the OEP method determines a local exchange potential uniquely, provided that we impose some appropriate boundary condition upon the exchange potential. When the number of orbitals is finite, however, the OEP integral equation is ill-posed in that it has an infinite number of solutions. We circumvent this problem by projecting the equation and the exchange potential upon the function space accessible by the kernel and thereby making the exchange potential unique. The observed numerical problems are, therefore, primarily due to the slow convergence of the projected exchange potential with respect to the size of the expansion basis set for orbitals. Nonetheless, by making a judicious choice of the basis sets, we obtain accurate exchange potentials for atoms and molecules from an LCAO OEP procedure, which are significant improvements over local or gradient-corrected exchange functionals or the Slater potential. The Krieger–Li–Iafrate scheme offers better approximations to the OEP method.
© 2001 American Institute of Physics. [DOI: 10.1063/1.1381013]

I. INTRODUCTION

There has been a resurrected interest in the optimized effective potential (OEP) method^{1,2} in connection with Kohn–Sham (KS) density functional theory (DFT).^{3–5} The OEP method, which involves a one-particle equation with an energy-independent and local (multiplicative) effective exchange potential in contrast with a non-local Hartree–Fock (HF) exchange integral operator, is inherently first principles in that it invokes an explicitly orbital-dependent expression of the exchange energy and hence offers a way to find a rigorous exchange potential within the KS DFT framework.^{6,7} The local exchange potential obtained from the OEP method possesses many of the analytical features of the exact KS potential.⁸ It has the correct $-1/r$ asymptotic behavior,² cancels exactly the self-interaction contribution to the Hartree potential, exhibits an integer discontinuity^{9–11} upon addition of an infinitesimal fraction of an electron to the highest occupied orbital, obeys the exchange virial theorem,^{12,13} yields the highest occupied orbital energy that satisfies Koopmans’ theorem, and is exact in the homogeneous-electron-gas limit. The local exchange potentials generated from the OEP method, which can be plotted

and visualized, will be instrumental in developing accurate and systematically improvable exchange functionals. This strategy may also be extended to correlation functionals by considering the question of finding energy independent and local effective potentials associated with some correlation energy expressions established in the wave function theory.^{11,14–26} This constitutes a paradigm of “*ab initio* density functional theory” advocated by one of the authors.²⁷

A critical element in performing *ab initio* density functional calculations and thereby obtaining accurate and systematically improvable exchange and correlation potentials is the ability to carry out the OEP calculations in the standard basis sets for quantum chemical applications, primarily Gaussian basis sets, and this raises the issue of numerical algorithms. Recently, we have developed a linear-combination-of-atomic-orbital (LCAO) algorithm for the OEP calculations of atoms and molecules,²⁸ on the basis of the finite-basis-set OEP formalism of Görling and Levy.^{18,19} A closely related LCAO OEP algorithm has also been reported by Görling.²⁹ These LCAO OEP methods permit OEP calculations of atoms and molecules on an equal footing to the conventional molecular orbital or density functional calculations, i.e., with conventional Gaussian-type basis sets, but without any further approximation. Thus, they extend the applicability of the OEP method, which had only been feasible for spherical (atomic) systems with grid-based

^{a)}Permanent address: Institute of Physics, Nicholas Copernicus University, Toruń, Poland.

^{b)}Author to whom correspondence should be addressed.

algorithms^{2,8,23,30-40} and for crystalline solids with plane-wave-based algorithms.⁴¹⁻⁴⁶

With these LCAO OEP methods, it is in principle possible to extract local exchange potentials and other properties from the OEP calculations of atoms and molecules. However, in the course of doing so, we encountered some numerical problems that appeared to indicate the existence of either formal or computational problems in the LCAO OEP method. For instance, the orbital energies directly obtained as the eigenvalues of the effective Fock matrix of the LCAO OEP method are excessively displaced from those of the correct OEP orbital energies (when available). The exchange potentials obtained from the LCAO OEP method are frequently unrealistic in that they tend to exhibit wrong asymptotic behavior (although formally they should have the correct asymptotic behavior) and also assume unphysical rapid oscillations around the nuclei. Within the LCAO framework, these unphysical solutions satisfy the OEP equation and self-consistency condition within reasonable numerical precision.

The purpose of this paper is to disclose and analyze these computational difficulties in the LCAO OEP method. The analysis leads to the title question which we attempt to answer from both formal and computational viewpoints. We give an algebraic proof that, with an infinity of orbitals, the kernel of the OEP integral equation has one and only one singularity associated with an additive constant and hence the OEP method determines a local exchange potential uniquely up to a constant. This indeterminacy can be eliminated readily by imposing some appropriate boundary condition on the exchange potential. When the number of orbitals is finite, however, the OEP integral equation is ill-posed in that it has an infinite number of solutions. We circumvent this problem by projecting the equation and the exchange potential upon the function space accessible by the kernel and thereby making the exchange potential unique. We ascribe the observed numerical problems primarily to the slow convergence of the projected exchange potential with respect to the size of the expansion basis set for orbitals; the basis-set incompleteness has a much more profound effect on the LCAO OEP method than on other SCF procedures such as the HF method. We demonstrate that, despite these computational problems, by making a judicious choice of the basis sets, we can obtain reasonably accurate exchange potentials for atoms and molecules from the LCAO OEP procedure, which are improvements over the exchange potentials obtained from some local or gradient-corrected functional or the Slater potentials,⁴⁷ yet are approximated well by the Krieger-Li-Iafrate (KLI) potentials.^{1,8,34,35,48,49}

II. FORMAL ASPECT

The purpose of this section is to prove that an exchange potential of an atomic or molecular system with a nondegenerate ground state can be uniquely determined up to a constant by the OEP equation alone. The same conclusion was drawn earlier by Görling and Levy,¹⁸ who considered the same problem from a different perspective (see also Ref. 24 for the uniqueness of the OEP orbitals). Here we confine our analysis to the exchange-only OEP method and do not con-

sider any correlation treatment, although our analysis may be extended to a correlated OEP method straightforwardly (see, however, Ref. 23 for a necessary condition for the existence of a solution). The OEP equation, which projects a nonlocal HF exchange operator onto a variationally optimal local exchange potential, was derived originally by Sharp and Horton¹ and by Talman and Shadwick² and rederived from a different viewpoint by Sham and Schlüter¹¹ and by Görling and Levy.^{18,19} For the σ -spin component of an exchange potential $V_{X\sigma}^{\text{OEP}}(\mathbf{r})$ (note that the exchange energy is separable into the α - and β -spin components and so is the exchange potential), the equation reads

$$\int X_{\sigma}(\mathbf{r}_1, \mathbf{r}_2) V_{X\sigma}^{\text{OEP}}(\mathbf{r}_2) d\mathbf{r}_2 = -2 \sum_{i,j}^{\text{occ}} \sum_a^{\text{virt}} \langle i_{\sigma} j_{\sigma} | j_{\sigma} a_{\sigma} \rangle \frac{\psi_{i\sigma}(\mathbf{r}_1) \psi_{a\sigma}(\mathbf{r}_1)}{\epsilon_{i\sigma} - \epsilon_{a\sigma}}, \quad (1)$$

where we designate σ -spin canonical OEP orbitals by $\{\psi_{p\sigma}(\mathbf{r})\}$, which we assume to be real for the sake of simplicity, σ -spin one-electron energies by $\{\epsilon_{p\sigma}\}$, and two-electron integrals in Dirac's notation,

$$\langle p_{\sigma} q_{\sigma} | r_{\sigma} s_{\sigma} \rangle = \int \int \frac{\psi_{p\sigma}(\mathbf{r}_1) \psi_{q\sigma}(\mathbf{r}_2) \psi_{r\sigma}(\mathbf{r}_1) \psi_{s\sigma}(\mathbf{r}_2)}{|\mathbf{r}_1 - \mathbf{r}_2|} d\mathbf{r}_1 d\mathbf{r}_2. \quad (2)$$

Equation (1) is a Fredholm integral equation of the first kind,^{50,51} and the numerical solution of such equations is notoriously unstable (see the next section). In this section, we assume that the set of all the orbitals forms the complete space, i.e.,

$$\sum_i^{\text{occ}} \psi_{i\sigma}(\mathbf{r}_1) \psi_{i\sigma}(\mathbf{r}_2) + \sum_a^{\text{virt}} \psi_{a\sigma}(\mathbf{r}_1) \psi_{a\sigma}(\mathbf{r}_2) = \delta(\mathbf{r}_1 - \mathbf{r}_2). \quad (3)$$

In the above equations and in the following, we use the convention that i, j, k label occupied orbitals, a, b label virtual orbitals, and p, q, r, s label either. The first factor in the integrand in Eq. (1) is the σ -spin part of the kernel,

$$X_{\sigma}(\mathbf{r}_1, \mathbf{r}_2) = 2 \sum_i^{\text{occ}} \sum_a^{\text{virt}} \frac{\psi_{i\sigma}(\mathbf{r}_1) \psi_{a\sigma}(\mathbf{r}_1) \psi_{i\sigma}(\mathbf{r}_2) \psi_{a\sigma}(\mathbf{r}_2)}{\epsilon_{i\sigma} - \epsilon_{a\sigma}}, \quad (4)$$

which is symmetric and separable (degenerate).^{50,51} We require that the exchange potential $V_{X\sigma}^{\text{OEP}}(\mathbf{r})$ satisfy Eq. (1) and the self-consistency condition between the canonical OEP orbitals and the exchange potential, i.e.,

$$\left\{ -\frac{1}{2} \nabla^2 + V_{\text{ext}}(\mathbf{r}_1) + \int \frac{\rho(\mathbf{r}_2)}{|\mathbf{r}_1 - \mathbf{r}_2|} d\mathbf{r}_2 + V_{X\sigma}^{\text{OEP}}(\mathbf{r}_1) \right\} \psi_{p\sigma}(\mathbf{r}_1) = \epsilon_p \psi_{p\sigma}(\mathbf{r}_1) \quad (\forall p), \quad (5)$$

simultaneously, where $V_{\text{ext}}(\mathbf{r})$ represents an external potential, which is typically an attractive potential produced by nuclei, and $\rho(\mathbf{r})$ is the electron density. We may formally isolate the exchange potential by rewriting Eq. (1) as

$$V_{X\sigma}^{\text{OEP}}(\mathbf{r}_1) = -2 \sum_{i,j}^{\text{occ}} \sum_a^{\text{virt}} \int \langle i_{\sigma} j_{\sigma} | j_{\sigma} a_{\sigma} \rangle \times \frac{\psi_{i\sigma}(\mathbf{r}_2) \psi_{a\sigma}(\mathbf{r}_2)}{\epsilon_{i\sigma} - \epsilon_{a\sigma}} X_{\sigma}^{-1}(\mathbf{r}_1, \mathbf{r}_2) d\mathbf{r}_2, \quad (6)$$

by introducing the inverse of the kernel $X_{\sigma}^{-1}(\mathbf{r}_1, \mathbf{r}_2)$, which must satisfy

$$\int X_{\sigma}^{-1}(\mathbf{r}_1, \mathbf{r}_2) X_{\sigma}(\mathbf{r}_2, \mathbf{r}_3) d\mathbf{r}_2 = \int X_{\sigma}(\mathbf{r}_1, \mathbf{r}_2) X_{\sigma}^{-1}(\mathbf{r}_2, \mathbf{r}_3) d\mathbf{r}_2 = \delta(\mathbf{r}_1 - \mathbf{r}_3), \quad (7)$$

although, as we shall show in the following, Eqs. (6) and (7) are mathematically ill-defined, as the kernel is not invertible.

The exchange potential $V_{X\sigma}^{\text{OEP}}(\mathbf{r})$ as defined by Eq. (1) alone is not necessarily unique, but there can be more than one such potential that satisfies this equation. This indeterminacy arises from the fact that the kernel $X_{\sigma}(\mathbf{r}_1, \mathbf{r}_2)$ is singular and is hence not invertible. We mean by saying that $X_{\sigma}(\mathbf{r}_1, \mathbf{r}_2)$ is singular that there are such functions $\{f(\mathbf{r})\}$ that satisfy the following condition pointwise:

$$\int X_{\sigma}(\mathbf{r}_1, \mathbf{r}_2) f(\mathbf{r}_2) d\mathbf{r}_2 = 0. \quad (8)$$

We call the space spanned by all those functions $\{f(\mathbf{r})\}$ that satisfy the above equation the null space of $X_{\sigma}(\mathbf{r}_1, \mathbf{r}_2)$ and a function that belongs to the null space is a null-space function. Suppose that we find a particular solution $V_{X\sigma}(\mathbf{r})$ that satisfies Eq. (1). When $X_{\sigma}(\mathbf{r}_1, \mathbf{r}_2)$ is singular and there is such a function $f(\mathbf{r})$ that satisfies Eq. (8), $V_{X\sigma}(\mathbf{r}) + f(\mathbf{r})$ is another solution of Eq. (1). This is readily understood by substituting $V_{X\sigma}(\mathbf{r}) + f(\mathbf{r})$ into Eq. (1). In the following, we shall demonstrate that $X_{\sigma}(\mathbf{r}_1, \mathbf{r}_2)$ has one and only one singularity with the associated null-space function being a constant, and hence that Eq. (1) alone can uniquely determine an exchange potential up to an additive constant. From Eq. (8), we find that any null-space function must satisfy

$$\int \int f(\mathbf{r}_1) X_{\sigma}(\mathbf{r}_1, \mathbf{r}_2) f(\mathbf{r}_2) d\mathbf{r}_1 d\mathbf{r}_2 = 0. \quad (9)$$

Substituting Eq. (4) into Eq. (9), we obtain

$$\sum_i^{\text{occ}} \sum_a^{\text{virt}} \frac{2}{\epsilon_{i\sigma} - \epsilon_{a\sigma}} \int \psi_{i\sigma}(\mathbf{r}_1) \psi_{a\sigma}(\mathbf{r}_1) f(\mathbf{r}_1) d\mathbf{r}_1 \int \psi_{i\sigma}(\mathbf{r}_2) \times \psi_{a\sigma}(\mathbf{r}_2) f(\mathbf{r}_2) d\mathbf{r}_2 = 0 \quad (\forall i, \forall a). \quad (10)$$

Since the denominator $\epsilon_{i\sigma} - \epsilon_{a\sigma}$ is negative, it is necessary that

$$\int \psi_{i\sigma}(\mathbf{r}) \psi_{a\sigma}(\mathbf{r}) f(\mathbf{r}) d\mathbf{r} = 0 \quad (\forall i, \forall a). \quad (11)$$

Suppose that there is only one occupied orbital, then $\psi_{i\sigma}(\mathbf{r}) f(\mathbf{r})$ is orthogonal to all the virtual orbitals $\{\psi_{a\sigma}(\mathbf{r})\}$ and is therefore a multiple of $\psi_{i\sigma}(\mathbf{r})$,

$$f(\mathbf{r}) \psi_{i\sigma}(\mathbf{r}) = c \psi_{i\sigma}(\mathbf{r}). \quad (12)$$

As we can safely assume that the lowest occupied orbital is nodeless and has a nonvanishing amplitude everywhere, we then divide both sides of Eq. (12) by $\psi_{i\sigma}(\mathbf{r})$ to obtain

$$f(\mathbf{r}) = c \quad (\text{constant}). \quad (13)$$

More generally, $\psi_{i\sigma}(\mathbf{r}) f(\mathbf{r})$ is expressed as a linear combination of all the occupied orbitals of $\{\psi_{i\sigma}(\mathbf{r})\}$,

$$f(\mathbf{r}) \psi_{i\sigma}(\mathbf{r}) = \sum_j^{\text{occ}} c_{ij} \psi_{j\sigma}(\mathbf{r}) \quad (\forall i), \quad (14)$$

with

$$c_{ij} = \int \psi_{j\sigma}(\mathbf{r}) f(\mathbf{r}) \psi_{i\sigma}(\mathbf{r}) d\mathbf{r}. \quad (15)$$

As the coefficients $\{c_{ij}\}$ are symmetric ($c_{ij} = c_{ji}$), we can find a symmetric transformation that brings these coefficients into a diagonal form,

$$\sum_i^{\text{occ}} u_{ki} c_{ij} = \lambda_k u_{kj}. \quad (16)$$

Multiplying u_{ki} on both sides of Eq. (14) and making the summation over i , we obtain

$$f(\mathbf{r}) \tilde{\psi}_{k\sigma}(\mathbf{r}) = \lambda_k \tilde{\psi}_{k\sigma}(\mathbf{r}) \quad (\forall k), \quad (17)$$

with

$$\tilde{\psi}_{k\sigma}(\mathbf{r}) = \sum_j^{\text{occ}} u_{kj} \psi_{j\sigma}(\mathbf{r}). \quad (18)$$

Since the transformed occupied orbitals $\{\tilde{\psi}_{i\sigma}(\mathbf{r})\}$ are nonvanishing everywhere except on two-dimensional nodal surfaces and an exchange potential is continuous, we can divide the both sides of Eq. (17) by $\tilde{\psi}_{k\sigma}(\mathbf{r})$ and obtain $f(\mathbf{r}) = c$ (constant). Thus, we conclude that an exchange potential of the OEP method can be uniquely determined up to an additive constant c from Eq. (1) alone. The sum of any particular solution of Eq. (1) and a constant simultaneously satisfies Eq. (1) and the self-consistency condition (5), and is hence another legitimate solution of an OEP problem. The additive constant can, however, be eliminated readily by imposing some appropriate boundary condition to the exchange potential, e.g.,

$$\lim_{r \rightarrow \infty} V_{X\sigma}^{\text{OEP}}(\mathbf{r}) = 0. \quad (19)$$

In this sense, the exchange potentials of the OEP method are essentially unique. It should be emphasized, however, that since $X_{\sigma}(\mathbf{r}_1, \mathbf{r}_2)$ is singular and is not invertible (although the nullity is just one), such expressions as Eqs. (6) and (7) are mathematically ill-defined unless the domain in which $X_{\sigma}^{-1}(\mathbf{r}_1, \mathbf{r}_2)$ is defined is chosen appropriately. Note also that the mathematical proof of uniqueness of the potential in regions far from nuclei depends on division by orbitals which are exponentially small.

In the next section, we shall invoke some properties that the exchange potentials of the OEP method possess, to judge how accurately the potentials obtained from the LCAO OEP

calculations reproduce the true solutions of the OEP method. First, for the highest occupied orbital $\psi_{N\sigma}(\mathbf{r})$ of each spin symmetry, we have

$$\int \psi_{N\sigma}(\mathbf{r}) V_{X\sigma}^{\text{OEP}}(\mathbf{r}) \psi_{N\sigma}(\mathbf{r}) d\mathbf{r} = - \sum_j^{\text{occ}} \langle N_{\sigma} j_{\sigma} | j_{\sigma} N_{\sigma} \rangle. \quad (20)$$

The derivation of this relationship, which we call the HOMO condition in the following, can be found elsewhere.⁸ Second, an exchange energy and potential of the OEP method obey the so-called exchange virial theorem of Ghosh and Parr¹² and of Levy and Perdew,¹³

$$E_{X\sigma}^{\text{OEP}} = - \frac{1}{2} \sum_{i,j} \langle i_{\sigma} j_{\sigma} | j_{\sigma} i_{\sigma} \rangle \\ = \int V_{X\sigma}^{\text{OEP}}(\mathbf{r}) \{3\rho_{\sigma}(\mathbf{r}) + \mathbf{r} \cdot \nabla \rho_{\sigma}(\mathbf{r})\} d\mathbf{r}, \quad (21)$$

where $\rho_{\sigma}(\mathbf{r})$ is the σ -spin electron density. Third, for one- and spin-unpolarized two-electron systems, there is an analytical solution to the OEP problem,

$$V_{X\sigma}^{\text{OEP}}(\mathbf{r}_1) = - \int \frac{\rho_{\sigma}(\mathbf{r}_2)}{|\mathbf{r}_1 - \mathbf{r}_2|} d\mathbf{r}_2 = - \int \frac{\psi_{i\sigma}(\mathbf{r}_2) \psi_{i\sigma}(\mathbf{r}_2)}{|\mathbf{r}_1 - \mathbf{r}_2|} d\mathbf{r}_2, \quad (22)$$

which reflects the fact that for these systems the exchange potential is just the self-interaction correction to the Hartree potential. It is straightforward to reduce the OEP equation (1) to the above simplified form for one- and spin-unpolarized two-electron systems.

III. COMPUTATIONAL ASPECT

A. The linear-combination-of-atomic-orbital optimized effective potential method and its algorithms

In the limit of an infinite basis set, the products of all the occupied and virtual orbitals $\{\psi_{i\sigma}(\mathbf{r}) \psi_{a\sigma}(\mathbf{r})\}$ essentially span the complete space with the only function that cannot be expanded by this set being a constant, and hence $X_{\sigma}(\mathbf{r}_1, \mathbf{r}_2)$ has only one singularity. In an LCAO OEP calculation, which employs a basis set of finite size to expand orbitals, $\{\psi_{i\sigma}(\mathbf{r}) \psi_{a\sigma}(\mathbf{r})\}$ is generally far from being a complete set, and the finite-basis-set representation of $X_{\sigma}(\mathbf{r}_1, \mathbf{r}_2)$, which we call the kernel matrix, has singularities, whose corresponding null-space functions are not necessarily an additive constant. Consequently, Eq. (1) alone can no longer uniquely determine an exchange potential, but it generates a set of exchange potentials that differ from each other by null-space functions of the kernel matrix (see p. 302 of Ref. 51).

Nonetheless, Eq. (1) alone can uniquely specify the projection of the exchange potentials onto the space spanned by $\{\psi_{i\sigma}(\mathbf{r}) \psi_{a\sigma}(\mathbf{r})\}$ (see p. 23 of Ref. 50),

$$\tilde{V}_{X\sigma}^{\text{OEP}}(\mathbf{r}_1) = \sum_{\kappa} \tilde{\theta}_{\kappa}(\mathbf{r}_1) \int \tilde{\theta}_{\kappa}(\mathbf{r}_2) V_{X\sigma}^{\text{OEP}}(\mathbf{r}_2) d\mathbf{r}_2, \quad (23)$$

where $\{\tilde{\theta}_{\kappa}\}$ denotes a set of basis functions that are orthonormal,

$$\int \tilde{\theta}_{\kappa}(\mathbf{r}) \tilde{\theta}_{\lambda}(\mathbf{r}) d\mathbf{r} = \delta_{\kappa\lambda}, \quad (24)$$

and span the same space as $\{\psi_{i\sigma}(\mathbf{r}) \psi_{a\sigma}(\mathbf{r})\}$,

$$\sum_{\kappa} \tilde{\theta}_{\kappa}(\mathbf{r}_1) \tilde{\theta}_{\kappa}(\mathbf{r}_2) = \sum_i^{\text{occ}} \sum_a^{\text{virt}} \psi_{i\sigma}(\mathbf{r}_1) \psi_{a\sigma}(\mathbf{r}_1) \psi_{i\sigma}(\mathbf{r}_2) \psi_{a\sigma}(\mathbf{r}_2). \quad (25)$$

Note that the projector in Eq. (23) erases any contribution from the null-space functions in $V_{X\sigma}^{\text{OEP}}(\mathbf{r}_2)$. Similarly, within the space spanned by $\{\psi_{i\sigma}(\mathbf{r}) \psi_{a\sigma}(\mathbf{r})\}$, $X_{\sigma}(\mathbf{r}_1, \mathbf{r}_2)$ is considered nonsingular and invertible. Thus, the inverse of $X_{\sigma}(\mathbf{r}_1, \mathbf{r}_2)$ within the space of $\{\psi_{i\sigma}(\mathbf{r}) \psi_{a\sigma}(\mathbf{r})\}$ can be defined unambiguously by

$$\int \tilde{X}_{\sigma}^{-1}(\mathbf{r}_1, \mathbf{r}_2) \tilde{X}_{\sigma}(\mathbf{r}_2, \mathbf{r}_3) d\mathbf{r}_2 = \sum_{\kappa} \tilde{\theta}_{\kappa}(\mathbf{r}_1) \tilde{\theta}_{\kappa}(\mathbf{r}_3), \quad (26)$$

and

$$\tilde{X}_{\sigma}(\mathbf{r}_1, \mathbf{r}_2) = \sum_{\kappa, \lambda} \tilde{\theta}_{\kappa}(\mathbf{r}_1) \tilde{\theta}_{\lambda}(\mathbf{r}_2) \\ \times \int \int \tilde{\theta}_{\kappa}(\mathbf{r}_3) X_{\sigma}(\mathbf{r}_3, \mathbf{r}_4) \tilde{\theta}_{\lambda}(\mathbf{r}_4) d\mathbf{r}_3 d\mathbf{r}_4 \\ = \sum_{\kappa, \lambda} \tilde{\theta}_{\kappa}(\mathbf{r}_1) \tilde{\theta}_{\lambda}(\mathbf{r}_2) (\tilde{\mathbf{X}}_{\sigma})_{\kappa\lambda}, \quad (27)$$

$$\tilde{X}_{\sigma}^{-1}(\mathbf{r}_1, \mathbf{r}_2) = \sum_{\kappa, \lambda} \tilde{\theta}_{\kappa}(\mathbf{r}_1) \tilde{\theta}_{\lambda}(\mathbf{r}_2) \\ \times \int \int \tilde{\theta}_{\kappa}(\mathbf{r}_3) X_{\sigma}^{-1}(\mathbf{r}_3, \mathbf{r}_4) \tilde{\theta}_{\lambda}(\mathbf{r}_4) d\mathbf{r}_3 d\mathbf{r}_4 \\ = \sum_{\kappa, \lambda} \tilde{\theta}_{\kappa}(\mathbf{r}_1) \tilde{\theta}_{\lambda}(\mathbf{r}_2) (\tilde{\mathbf{X}}_{\sigma}^{-1})_{\kappa\lambda}. \quad (28)$$

Note that $X_{\sigma}^{-1}(\mathbf{r}_1, \mathbf{r}_2)$ is an ill-defined quantity, but $\tilde{X}_{\sigma}^{-1}(\mathbf{r}_1, \mathbf{r}_2)$ is not, and hence the matrix representation of the latter, $\tilde{\mathbf{X}}_{\sigma}^{-1}$, can be obtained as the inverse of the kernel matrix $\tilde{\mathbf{X}}_{\sigma}$. With the aid of this projector, we can recast Eq. (6) into a well-defined equation for $\tilde{V}_{X\sigma}^{\text{OEP}}(\mathbf{r})$ as

$$\tilde{V}_{X\sigma}^{\text{OEP}}(\mathbf{r}_1) = -2 \sum_{i,j}^{\text{occ}} \sum_a^{\text{virt}} \int \langle i_{\sigma} j_{\sigma} | j_{\sigma} a_{\sigma} \rangle \\ \times \frac{\psi_{i\sigma}(\mathbf{r}_2) \psi_{a\sigma}(\mathbf{r}_2)}{\epsilon_{i\sigma} - \epsilon_{a\sigma}} \tilde{X}_{\sigma}^{-1}(\mathbf{r}_1, \mathbf{r}_2) d\mathbf{r}_2. \quad (29)$$

Equations (26)–(29) are the basis of what we call the S algorithm of the LCAO OEP method.²⁸ The exchange potential is, therefore, expanded by $\{\tilde{\theta}_{\kappa}\}$ as

$$\tilde{V}_{X\sigma}^{\text{OEP}}(\mathbf{r}) = \sum_{\kappa} d_{\kappa} \tilde{\theta}_{\kappa}(\mathbf{r}), \quad (30)$$

where the expansion coefficients $\{d_{\kappa}\}$ are

$$d_{\kappa} = -2 \sum_{i,j}^{\text{occ}} \sum_a^{\text{virt}} \sum_{\lambda} \frac{\langle i_{\sigma} j_{\sigma} | j_{\sigma} a_{\sigma} \rangle}{\epsilon_{i\sigma} - \epsilon_{a\sigma}} (\tilde{\mathbf{X}}_{\sigma}^{-1})_{\kappa\lambda} \times \int \psi_{i\sigma}(\mathbf{r}) \psi_{a\sigma}(\mathbf{r}) \tilde{\theta}_{\lambda}(\mathbf{r}) d\mathbf{r}. \quad (31)$$

Alternatively, we may define the projector by

$$\tilde{V}_{X\sigma}^{\text{OEP}}(\mathbf{r}_1) = \sum_{\kappa} \int \int \frac{\tilde{\theta}_{\kappa}(\mathbf{r}_2) \tilde{\theta}_{\kappa}(\mathbf{r}_3) V_{X\sigma}^{\text{OEP}}(\mathbf{r}_3)}{|\mathbf{r}_1 - \mathbf{r}_2|} d\mathbf{r}_2 d\mathbf{r}_3, \quad (32)$$

where $\{\tilde{\theta}_{\kappa}\}$ are orthonormalized in such a fashion that

$$\int \int \frac{\tilde{\theta}_{\kappa}(\mathbf{r}_1) \tilde{\theta}_{\lambda}(\mathbf{r}_2)}{|\mathbf{r}_1 - \mathbf{r}_2|} d\mathbf{r}_1 d\mathbf{r}_2 = \delta_{\kappa\lambda}, \quad (33)$$

and also that they span the same space as $\{\psi_{i\sigma}(\mathbf{r}) \psi_{a\sigma}(\mathbf{r})\}$, i.e.,

$$\sum_{\kappa} \int \frac{\tilde{\theta}_{\kappa}(\mathbf{r}_2) \tilde{\theta}_{\kappa}(\mathbf{r}_3)}{|\mathbf{r}_1 - \mathbf{r}_2|} d\mathbf{r}_2 = \sum_i^{\text{occ}} \sum_a^{\text{virt}} \psi_{i\sigma}(\mathbf{r}_1) \psi_{a\sigma}(\mathbf{r}_1) \psi_{i\sigma}(\mathbf{r}_3) \psi_{a\sigma}(\mathbf{r}_3). \quad (34)$$

With these biorthogonal basis functions, a rational definition of $X_{\sigma}(\mathbf{r}_1, \mathbf{r}_2)$ and $X_{\sigma}^{-1}(\mathbf{r}_1, \mathbf{r}_2)$ within the space of $\{\psi_{i\sigma}(\mathbf{r}) \psi_{a\sigma}(\mathbf{r})\}$ would be

$$\int \tilde{X}_{\sigma}^{-1}(\mathbf{r}_1, \mathbf{r}_2) \tilde{X}_{\sigma}(\mathbf{r}_2, \mathbf{r}_3) d\mathbf{r}_2 = \sum_{\kappa} \int \frac{\tilde{\theta}_{\kappa}(\mathbf{r}_2) \tilde{\theta}_{\kappa}(\mathbf{r}_3)}{|\mathbf{r}_1 - \mathbf{r}_2|} d\mathbf{r}_2 \quad (35)$$

and

$$\begin{aligned} \tilde{X}_{\sigma}(\mathbf{r}_1, \mathbf{r}_2) &= \sum_{\kappa, \lambda} \tilde{\theta}_{\kappa}(\mathbf{r}_1) \tilde{\theta}_{\lambda}(\mathbf{r}_2) \\ &\times \int \int \int \int \frac{\tilde{\theta}_{\kappa}(\mathbf{r}_3) X_{\sigma}(\mathbf{r}_4, \mathbf{r}_5) \tilde{\theta}_{\lambda}(\mathbf{r}_6)}{|\mathbf{r}_3 - \mathbf{r}_4| |\mathbf{r}_5 - \mathbf{r}_6|} \\ &\times d\mathbf{r}_3 d\mathbf{r}_4 d\mathbf{r}_5 d\mathbf{r}_6 \\ &= \sum_{\kappa, \lambda} \tilde{\theta}_{\kappa}(\mathbf{r}_1) \tilde{\theta}_{\lambda}(\mathbf{r}_2) (\tilde{\mathbf{X}}_{\sigma})_{\kappa\lambda}, \end{aligned} \quad (36)$$

$$\begin{aligned} \tilde{X}_{\sigma}^{-1}(\mathbf{r}_1, \mathbf{r}_2) &= \sum_{\kappa, \lambda} \int \int \frac{\tilde{\theta}_{\kappa}(\mathbf{r}_3) \tilde{\theta}_{\lambda}(\mathbf{r}_4)}{|\mathbf{r}_1 - \mathbf{r}_3| |\mathbf{r}_2 - \mathbf{r}_4|} d\mathbf{r}_3 d\mathbf{r}_4 \\ &\times \int \int \tilde{\theta}_{\kappa}(\mathbf{r}_5) X_{\sigma}^{-1}(\mathbf{r}_5, \mathbf{r}_6) \tilde{\theta}_{\lambda}(\mathbf{r}_6) d\mathbf{r}_5 d\mathbf{r}_6 \\ &= \sum_{\kappa, \lambda} \int \int \frac{\tilde{\theta}_{\kappa}(\mathbf{r}_3) \tilde{\theta}_{\lambda}(\mathbf{r}_4)}{|\mathbf{r}_1 - \mathbf{r}_3| |\mathbf{r}_2 - \mathbf{r}_4|} d\mathbf{r}_3 d\mathbf{r}_4 (\tilde{\mathbf{X}}_{\sigma}^{-1})_{\kappa\lambda}. \end{aligned} \quad (37)$$

Again, the matrix $\tilde{\mathbf{X}}_{\sigma}^{-1}$ is simply the inverse of $\tilde{\mathbf{X}}_{\sigma}$. The exchange potential is, in this case, represented as an electrostatic potential created by a charge density which is in turn expanded by $\{\tilde{\theta}_{\kappa}\}$. Therefore,

$$\tilde{V}_{X\sigma}^{\text{OEP}}(\mathbf{r}_1) = \sum_{\kappa} d_{\kappa} \int \frac{\tilde{\theta}_{\kappa}(\mathbf{r}_2)}{|\mathbf{r}_1 - \mathbf{r}_2|} d\mathbf{r}_2, \quad (38)$$

and the expansion coefficients $\{d_{\kappa}\}$ are

$$d_{\kappa} = -2 \sum_{i,j}^{\text{occ}} \sum_a^{\text{virt}} \sum_{\lambda} \frac{\langle i_{\sigma} j_{\sigma} | j_{\sigma} a_{\sigma} \rangle}{\epsilon_{i\sigma} - \epsilon_{a\sigma}} (\tilde{\mathbf{X}}_{\sigma}^{-1})_{\kappa\lambda} \times \int \int \frac{\psi_{i\sigma}(\mathbf{r}_1) \psi_{a\sigma}(\mathbf{r}_1) \tilde{\theta}_{\lambda}(\mathbf{r}_2)}{|\mathbf{r}_1 - \mathbf{r}_2|} d\mathbf{r}_1 d\mathbf{r}_2. \quad (39)$$

The above equations are the basis of the V algorithm of the LCAO OEP method.²⁹

In practice, we obtain the matrix $\tilde{\mathbf{X}}_{\sigma}^{-1}$ in the following procedure. We first expand the operator $X_{\sigma}(\mathbf{r}_1, \mathbf{r}_2)$ by a set of orthonormal basis functions $\{\theta_{\kappa}\}$ as

$$X_{\sigma}(\mathbf{r}_1, \mathbf{r}_2) \approx \sum_{\kappa, \lambda} \theta_{\kappa}(\mathbf{r}_1) \theta_{\lambda}(\mathbf{r}_2) (\mathbf{X}_{\sigma})_{\kappa\lambda} \quad (40)$$

and

$$(\mathbf{X}_{\sigma})_{\kappa\lambda} = \int \int \theta_{\kappa}(\mathbf{r}_1) X_{\sigma}(\mathbf{r}_1, \mathbf{r}_2) \theta_{\lambda}(\mathbf{r}_2) d\mathbf{r}_1 d\mathbf{r}_2 \quad (41)$$

$$\begin{aligned} &= \sum_i^{\text{occ}} \sum_a^{\text{virt}} \frac{2}{\epsilon_{i\sigma} - \epsilon_{a\sigma}} \int \psi_{i\sigma}(\mathbf{r}_1) \psi_{a\sigma}(\mathbf{r}_1) \theta_{\kappa}(\mathbf{r}_1) d\mathbf{r}_1 \\ &\times \int \psi_{i\sigma}(\mathbf{r}_2) \psi_{a\sigma}(\mathbf{r}_2) \theta_{\lambda}(\mathbf{r}_2) d\mathbf{r}_2 \end{aligned} \quad (42)$$

in the S algorithm or

$$(\mathbf{X}_{\sigma})_{\kappa\lambda} = \int \int \int \int \frac{\theta_{\kappa}(\mathbf{r}_1) X_{\sigma}(\mathbf{r}_2, \mathbf{r}_3) \theta_{\lambda}(\mathbf{r}_4)}{|\mathbf{r}_1 - \mathbf{r}_2| |\mathbf{r}_3 - \mathbf{r}_4|} d\mathbf{r}_1 d\mathbf{r}_2 d\mathbf{r}_3 d\mathbf{r}_4 \quad (43)$$

$$\begin{aligned} &= \sum_i^{\text{occ}} \sum_a^{\text{virt}} \frac{2}{\epsilon_{i\sigma} - \epsilon_{a\sigma}} \\ &\times \int \int \frac{\psi_{i\sigma}(\mathbf{r}_1) \psi_{a\sigma}(\mathbf{r}_1) \theta_{\kappa}(\mathbf{r}_2)}{|\mathbf{r}_1 - \mathbf{r}_2|} d\mathbf{r}_1 d\mathbf{r}_2 \\ &\times \int \int \frac{\psi_{i\sigma}(\mathbf{r}_3) \psi_{a\sigma}(\mathbf{r}_3) \theta_{\lambda}(\mathbf{r}_4)}{|\mathbf{r}_3 - \mathbf{r}_4|} d\mathbf{r}_3 d\mathbf{r}_4, \end{aligned} \quad (44)$$

in the V algorithm. The basis set $\{\theta_{\kappa}\}$ is created by a canonical orthogonalization of a set of auxiliary Gaussian-type basis functions (the potential basis set) on the basis of the normalization defined either by Eq. (24) or (33). Hence, at this point, any linear dependence of the potential basis functions can be eliminated. As the matrix \mathbf{X}_{σ} is symmetric, we can find a symmetric matrix \mathbf{U} that diagonalizes \mathbf{X}_{σ} , i.e.,

$$\mathbf{X}_{\sigma} = \mathbf{U} \mathbf{W} \mathbf{U}^T, \quad (45)$$

where \mathbf{W} is a diagonal matrix and \mathbf{U}^T is the transpose of \mathbf{U} . Although \mathbf{X}_{σ} is negative-definite, generally the several least negative eigenvalues are computationally zero or very close to zero, despite the fact that the potential basis set is not capable of expressing an additive constant. These singularities of \mathbf{X}_{σ} must not be confused with the linear dependence of the potential basis set. The singularities occur owing to the fact that the potential basis functions can represent functions

in the null space of the matrix representation of $X_\sigma(\mathbf{r}_1, \mathbf{r}_2)$. The basis set $\{\tilde{\theta}_\kappa\}$ that is orthogonal to the null space of \mathbf{X}_σ can be generated by

$$\tilde{\theta}_\kappa = \sum_\lambda \tilde{U}_{\kappa\lambda} \theta_\lambda, \quad (46)$$

where \tilde{U} is a rectangular matrix obtained by eliminating any row of \mathbf{U} whose corresponding eigenvalue is less negative than a preset threshold. The matrix representation of $\tilde{X}_\sigma(\mathbf{r}_1, \mathbf{r}_2)$ and $\tilde{X}_\sigma^{-1}(\mathbf{r}_1, \mathbf{r}_2)$ within the basis set $\{\tilde{\theta}_\kappa\}$ would simply be

$$(\tilde{\mathbf{X}}_\sigma)_{\kappa\lambda} = \delta_{\kappa\lambda} w_\kappa, \quad (47)$$

$$(\tilde{\mathbf{X}}_\sigma^{-1})_{\kappa\lambda} = \delta_{\kappa\lambda} w_\kappa^{-1}. \quad (48)$$

Note that the dimensions of $\tilde{\mathbf{X}}_\sigma$ and $\tilde{\mathbf{X}}_\sigma^{-1}$ are reduced to the rank (the dimension minus the nullity) of \mathbf{X}_σ . This procedure amounts to the singular value decomposition of \mathbf{X}_σ .

In the LCAO OEP method, the pointwise self-consistency condition, Eq. (5), may not be satisfied. Instead, we require that the following condition

$$\int \psi_{p\sigma}(\mathbf{r}_1) \left\{ -\frac{1}{2} \nabla^2 + V_{\text{ext}}(\mathbf{r}_1) + \int \frac{\rho(\mathbf{r}_2)}{|\mathbf{r}_1 - \mathbf{r}_2|} d\mathbf{r}_2 + \tilde{V}_{X_\sigma}^{\text{OEP}}(\mathbf{r}_1) \right\} \times \psi_{q\sigma}(\mathbf{r}_1) d\mathbf{r}_1 = \delta_{pq} \epsilon_{p\sigma} \quad (\nabla p, \nabla q), \quad (49)$$

be fulfilled, with the constraint that the orbitals $\{\psi_{p\sigma}\}$ remain orthonormal

$$\int \psi_{p\sigma}(\mathbf{r}) \psi_{q\sigma}(\mathbf{r}) d\mathbf{r} = \delta_{pq}. \quad (50)$$

As usual, we express each orbital as a linear combination of atomic orbitals $\{\chi_\mu\}$

$$\psi_{p\sigma}(\mathbf{r}) = \sum_\mu C_{\mu p}^\sigma \chi_\mu(\mathbf{r}) \quad (\nabla p), \quad (51)$$

and we arrive at the Hartree–Fock–Roothaan-type matrix eigenvalue equation for the expansion coefficients,

$$\sum_\nu F_{\mu\nu}^\sigma C_{\nu p}^\sigma = \epsilon_{p\sigma} \sum_\nu S_{\mu\nu}^\sigma C_{\nu p}^\sigma \quad (\nabla p), \quad (52)$$

with

$$F_{\mu\nu}^\sigma = \int \chi_\mu(\mathbf{r}_1) \left\{ -\frac{1}{2} \nabla^2 + V_{\text{ext}}(\mathbf{r}_1) + \int \frac{\rho(\mathbf{r}_2)}{|\mathbf{r}_1 - \mathbf{r}_2|} d\mathbf{r}_2 + \tilde{V}_{X_\sigma}^{\text{OEP}}(\mathbf{r}_1) \right\} \chi_\nu(\mathbf{r}_1) d\mathbf{r}_1, \quad (53)$$

$$S_{\mu\nu}^\sigma = \int \chi_\mu(\mathbf{r}) \chi_\nu(\mathbf{r}) d\mathbf{r}. \quad (54)$$

The LCAO OEP methods with the S and V algorithms are implemented in the POLYMER program.⁵² When the S algorithm of the LCAO OEP method is employed, two- and three-center overlap integrals involving the auxiliary Gaussian functions are needed. In our implementation, these integrals are evaluated analytically by virtue of the Obara–Saika recursion formulas.⁵³ Thus, the effective Fock matrix ele-

ments of the OEP method can be evaluated analytically. In the V algorithm, we compute analytically two- and three-center electron-repulsion integrals involving the auxiliary Gaussian functions.^{53,54} The effective Fock matrix elements can be computed by these three-center electron repulsion integrals and the SCF procedure can be accomplished without any numerical quadrature. The integral in Eq. (38) can also be evaluated analytically with the recursion formulas for the nucleus–electron attraction integrals.⁵⁵

In the next section we also consider the Slater⁴⁷ and KLI potentials,^{1,8,34,35,48,49} which are implemented in the POLYMER program.⁵² The Slater potential $V_{X_\sigma}^{\text{Slater}}(\mathbf{r})$ is obtained by averaging the nonlocal HF exchange potential in a certain manner and is given by

$$V_{X_\sigma}^{\text{Slater}}(\mathbf{r}_1) = - \sum_{i,j}^{\text{occ}} \frac{\psi_{i\sigma}(\mathbf{r}_1) \psi_{j\sigma}(\mathbf{r}_1)}{\rho_\sigma(\mathbf{r}_1)} \int \frac{\psi_{i\sigma}(\mathbf{r}_2) \psi_{j\sigma}(\mathbf{r}_2)}{|\mathbf{r}_1 - \mathbf{r}_2|} d\mathbf{r}_2. \quad (55)$$

For one- and spin-unpolarized two-electron systems, the Slater potentials reduce to Eq. (22) and hence to the analytical solutions of the OEP equation. However, except for the one- and spin-unpolarized two-electron systems, the Slater potentials do not satisfy the HOMO condition expressed by Eq. (20). The KLI potential $V_{X_\sigma}^{\text{KLI}}(\mathbf{r})$ is defined as the sum of the Slater potential and a correction term,

$$V_{X_\sigma}^{\text{KLI}}(\mathbf{r}) = V_{X_\sigma}^{\text{Slater}}(\mathbf{r}) + \sum_i^{N_\sigma-1} \frac{\psi_{i\sigma}(\mathbf{r}) \psi_{i\sigma}(\mathbf{r})}{\rho_\sigma(\mathbf{r})} (\bar{V}_{X_{i\sigma}}^{\text{KLI}} - \bar{V}_{X_{i\sigma}}^{\text{HF}}), \quad (56)$$

where $\bar{V}_{X_{i\sigma}}^{\text{KLI}}$ and $\bar{V}_{X_{i\sigma}}^{\text{HF}}$ refer to the orbital expectation value of the respective potentials, i.e.,

$$\bar{V}_{X_{i\sigma}}^{\text{HF}} = - \sum_j^{\text{occ}} \langle i_\sigma j_\sigma | j_\sigma i_\sigma \rangle, \quad (57)$$

and the summation in Eq. (56) excludes the highest occupied orbital of each symmetry (N_σ is the number of σ -spin occupied orbitals). By also defining the orbital expectation value of the Slater potential as

$$\bar{V}_{X_{i\sigma}}^{\text{Slater}} = \int \psi_{i\sigma}(\mathbf{r}) V_{X_\sigma}^{\text{Slater}}(\mathbf{r}) \psi_{i\sigma}(\mathbf{r}) d\mathbf{r}, \quad (58)$$

we require that $\bar{V}_{X_{i\sigma}}^{\text{KLI}}$ be given by

$$\bar{V}_{X_{i\sigma}}^{\text{KLI}} = \bar{V}_{X_{i\sigma}}^{\text{Slater}} + \sum_j^{N_\sigma-1} M_{ij}^\sigma (\bar{V}_{X_{j\sigma}}^{\text{KLI}} - \bar{V}_{X_{j\sigma}}^{\text{HF}}), \quad (59)$$

with

$$M_{ij}^\sigma = \int \frac{\psi_{i\sigma}(\mathbf{r}) \psi_{i\sigma}(\mathbf{r}) \psi_{j\sigma}(\mathbf{r}) \psi_{j\sigma}(\mathbf{r})}{\rho_\sigma(\mathbf{r})} d\mathbf{r}. \quad (60)$$

The KLI potentials reduce to Eq. (22) for one- and spin-unpolarized two-electron systems and also satisfy the HOMO condition for any system.⁸ In the following, we plot the Slater and KLI potentials as a function of the coordinates of space. The integral in Eq. (55) can be evaluated analyti-

cally at each point of a numerical grid by the recursion formulas for the nucleus–electron attraction integrals.⁵⁵ The integrals (58) and (60) and also the exchange matrix elements of the LCAO KLI method are evaluated by numerical integration employing Becke's method (fuzzy cell method).⁵⁶ The numerical grid for this numerical quadrature is the same grid⁵⁷ that we use for the conventional LCAO DFT calculations and it consists of a second-kind Gauss–Chebyshev radial grid and Lebedev angular grids.^{58–60} The divisions in Eqs. (55), (56), and (60) can be carried out safely until the electron density decays and becomes computationally zero.

The right-hand side of Eq. (21) is evaluated by the numerical quadrature employing the same grid and the shifted exchange potential (vide post), electron density, and electron density gradients obtained from the converged LCAO OEP calculations.

B. Numerical results and discussion

In this section, we compute and plot the exchange potentials obtained from the LCAO OEP method with the S and V algorithms. We compare them against the Slater potential, the KLI potential, and the exchange potentials obtained from the local density approximation (LDA)⁶¹ to the exchange functional and Becke's gradient-corrected exchange functional (Becke88).⁶² These potentials are computed at each point of a numerical grid by using the orbitals, orbital energies, and electron densities obtained from the corresponding converged LCAO OEP calculations. It should be noted that the exchange potentials of the LCAO OEP method shown in all the figures in this paper are shifted by some constants (see

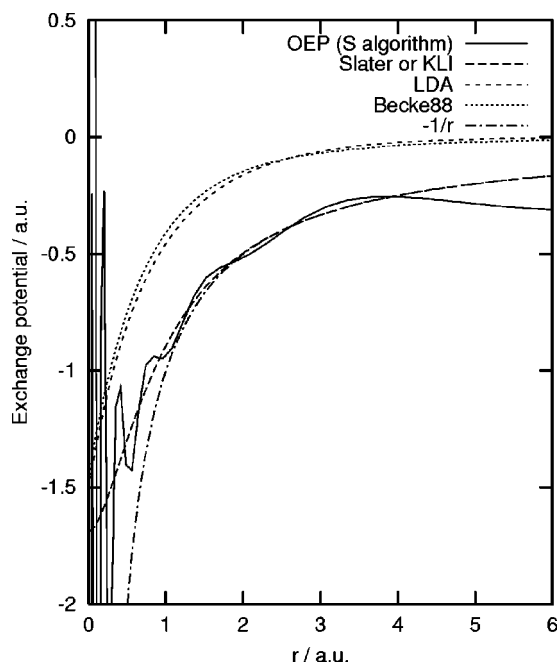


FIG. 1. The exchange potentials of the helium atom as a function of the distance from the nucleus (r). The orbital basis set (small) consists of 12 even-tempered s -type functions with the exponents given by 0.1×2^n ($0 \leq n \leq 11$) and the potential basis set (large) consists of 25 even-tempered s -type functions with the exponents given by 0.05×2^n ($0 \leq n \leq 24$). The exchange potential obtained from the S algorithm of the LCAO OEP method is shifted by -0.3118 a.u.

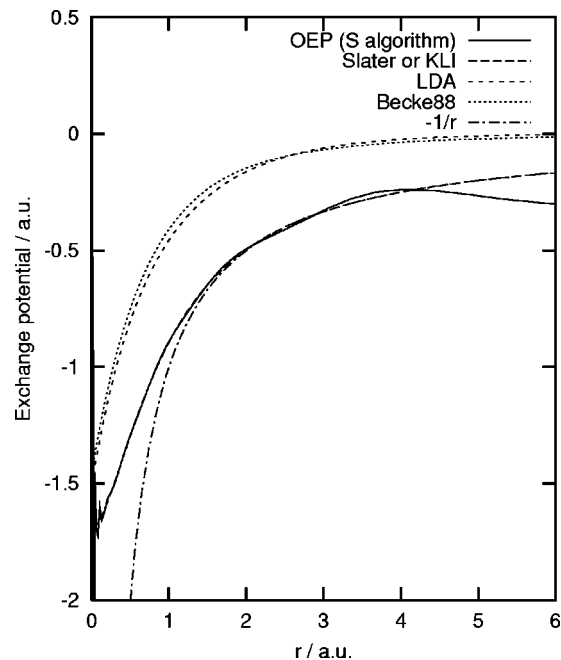


FIG. 2. The exchange potentials of the helium atom as a function of the distance from the nucleus (r). The orbital basis set (medium) consists of 20 even-tempered s -type functions with the exponents given by 0.1×2^n ($0 \leq n \leq 19$) and the potential basis set is the large basis set (see the caption of Fig. 1). The exchange potential obtained from the S algorithm of the LCAO OEP method is shifted by -0.3018 a.u.

the figure captions) so that the HOMO condition is satisfied when the left-hand side of Eq. (20) is evaluated for the shifted potentials. The potentials directly obtained from the LCAO OEP calculations are substantially displaced from the ones shown in the figures (although the shape of the potentials remains the same), and generally the HOMO condition is not satisfied for them. The total energies, exchange energies, and the highest occupied orbital energies obtained from these calculations are summarized in Table I, in which are also included the results of self-consistent LCAO LDA, LCAO Becke88, and LCAO KLI calculations.

As a first example, we choose the helium atom. For this two-electron system, the Slater and KLI potentials are identical to each other and also reduce to the analytical solution of the OEP equation. Thus, the comparison of the exchange potentials of the LCAO OEP method and the Slater or KLI potentials gives the definitive assessment of the quality of the former potentials. In Figs. 1–3, we plot the exchange potentials of the helium atom obtained from the S algorithm as a function of the distance from the nucleus (r) employing three different orbital basis sets, which we simply denote small, medium, and large basis sets, respectively, according to their size. We employ the large basis set for the potential basis set in these three calculations. The small, medium, and large basis sets consist, respectively, of 12, 20, and 25 even-tempered s -type functions, and since the helium atom has spherical symmetry, the addition of p -type functions and functions with higher angular momenta to the orbital or potential basis set will not alter the shape of the potential or the total energy.

We immediately notice from Fig. 1 that the exchange

TABLE I. Total ground-state energies (E), exchange energies (E_x), and the highest occupied orbital energies (ϵ_{HOMO}) computed by the HF, OEP, KLI, LDA, and Becke88 methods (in hartrees). The exchange energies given in the parentheses are obtained from the right-hand side of Eq. (21).

	Theory	Algorithm ^a	E	E_x	ϵ_{HOMO}	
He ^b	HF	LCAO/12s	-2.8614	-1.0257	-0.9179	
	OEP	LCAO- <i>S</i> /12s	-2.8614	-1.0257(-1.0277)	-0.6061	
	OEP	LCAO- <i>V</i> /12s	-2.8614	-1.0257(-1.0257)	-0.6981	
	KLI	LCAO/12s	-2.8614	-1.0257	-0.9179	
	LDA	LCAO/12s	-2.7234	-0.8527	-0.5169	
	Becke88	LCAO/12s	-2.8631	-1.0159	-0.5540	
	HF	LCAO/20s	-2.8617	-1.0258	-0.9180	
	OEP	LCAO- <i>S</i> /20s	-2.8617	-1.0258(-1.0259)	-0.6162	
	OEP	LCAO- <i>V</i> /20s	-2.8617	-1.0258(-1.0258)	-0.7049	
	KLI	LCAO/20s	-2.8617	-1.0258	-0.9180	
	LDA	LCAO/20s	-2.7236	-0.8528	-0.5169	
	Becke88	LCAO/20s	-2.8634	-1.0161	-0.5541	
	HF	LCAO/25s	-2.8617	-1.0258	-0.9180	
	OEP	LCAO- <i>S</i> /25s	-2.8617	-1.0258(-1.0258)	-0.6991	
	OEP	LCAO- <i>V</i> /25s	-2.8617	-1.0258(-1.0258)	-0.7647	
	KLI	LCAO/25s	-2.8617	-1.0258	-0.9180	
	LDA	LCAO/25s	-2.7236	-0.8528	-0.5170	
	Becke88	LCAO/25s	-2.8634	-1.0160	-0.5541	
	OEP	Grid	-2.8617 ^c	-1.0258 ^c	-0.9180 ^c	
H ₂ ^d	HF	LCAO	-1.1336	-0.6586	-0.5946	
	OEP	LCAO- <i>S</i>	-1.1336	-0.6586(-0.6583)	-0.3282	
	OEP	LCAO- <i>V</i>	-1.1336	-0.6586(-0.6585)	-0.4062	
	KLI	LCAO	-1.1336	-0.6586	-0.5946	
	LDA	LCAO	-1.0436	-0.5515	-0.3311	
	Becke88	LCAO	-1.1321	-0.6547	-0.3560	
		KLI	Grid	-1.1336 ^e		
Ne ^f	HF	LCAO	-128.5471	-12.1084	-0.8504	
	OEP	LCAO- <i>S</i>	-128.5454	-12.1050(-12.1048)	-0.6162	
	OEP	LCAO- <i>V</i>	-128.5454	-12.1050(-12.1046)	-0.7639	
	KLI	LCAO	-128.5448	-12.0991	-0.8494	
	LDA	LCAO	-127.4907	-10.9372	-0.4430	
	Becke88	LCAO	-128.5901	-12.0864	-0.4545	
		OEP	Grid	-128.5455 ^c	-12.1050 ^c	-0.8507 ^c
		KLI	Grid	-128.5448 ^g		-0.8494 ^g
N ₂ ^h	HF	LCAO	-108.9791	-13.0963	-0.6144	
	OEP	LCAO- <i>S</i>	-108.9741	-13.0859(-13.2857)	-0.3818	
	OEP	LCAO- <i>V</i>	-108.9738	-13.0858(-13.2026)	-1.0696	
	LDA	LCAO	-107.7438	-11.7839	-0.3348	
	Becke88	LCAO	-109.0730	-13.1872	-0.3462	
		KLI	Grid	-108.9853 ^e		
LiF ⁱ	HF	LCAO	-106.9810	-11.9973	-0.4763	
	OEP	LCAO- <i>S</i>	-106.9790	-11.9940(-12.0289)	-0.3775	
	OEP	LCAO- <i>V</i>	-106.9790	-11.9939(-11.9720)	-0.6743	
	LDA	LCAO	-105.8667	-10.7172	-0.1894	
	Becke88	LCAO	-107.0457	-11.9719	-0.1946	

^aGrid-based numerical algorithms provide basis-set-limit results.

^bSee the captions of Figs. 1–6 for the basis sets employed in the LCAO calculations.

^cReference 36.

^dSee the captions of Figs. 7 and 8 for the geometry and the basis sets employed in the LCAO calculations.

^eReference 68.

^fSee the captions of Figs. 9 and 10 for the basis sets employed.

^gReference 49.

^hSee the captions of Figs. 11 and 12 for the geometry and the basis sets employed in the LCAO calculations.

ⁱSee the captions of Figs. 13 and 14 for the geometry and the basis sets employed in the LCAO calculations.

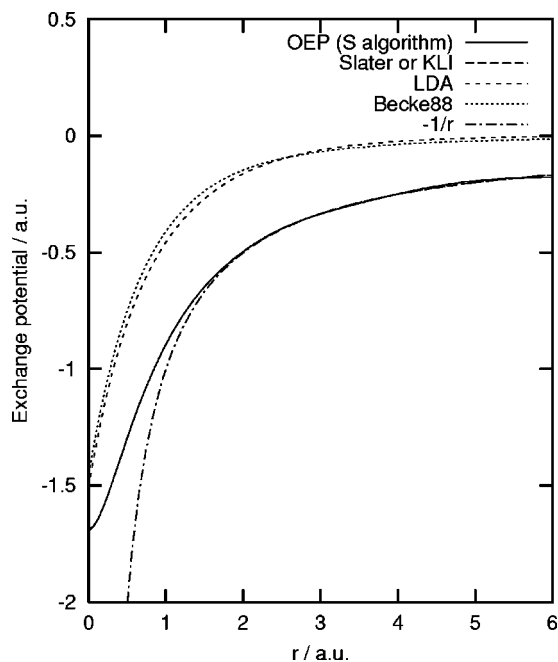


FIG. 3. The exchange potentials of the helium atom as a function of the distance from the nucleus (r). We employ the large basis set for the orbitals and the potential (see the caption of Fig. 1). The exchange potential obtained from the S algorithm of the LCAO OEP method is shifted by -0.2189 a.u. The OEP potential and the Slater or KLI potential are hardly discernible.

potential of the LCAO OEP method obtained with a rather small orbital basis set has several unrealistic characteristics. It wildly oscillates around the nucleus and it does not have the correct $-1/r$ asymptotic behavior. This is in contrast to the Slater or KLI potential that is exact (within the given orbital basis set) for this system and also smoothly merges into the curve of $-1/r$ at large r . Although the exchange potential of the LCAO OEP method in Fig. 1 is shifted downwards from the original by 0.31 a.u., the shifted potential appears to follow the trend of the Slater or KLI potential in the range of $0.5 < r < 4$. The shape of the LDA and Becke88 exchange potentials (but not the magnitude of them) is in reasonable agreement with that of the correct potential in the range of $0 < r < 2$, but the former potentials decay too rapidly, not having the correct $-1/r$ asymptotic behavior. Due to this lack of the correct asymptotic behavior, the LDA and Becke88 exchange potentials are too shallow in the whole range of r as compared with the correct potential. As we increase the size of the orbital basis set from small (Fig. 1) to medium (Fig. 2), the exchange potential of the LCAO OEP method becomes remarkably better in the sense that the potential closely resembles the correct potentials in the range of $0.3 < r < 2$. However, we can still observe a rapid oscillation of the potential around the nucleus and the wrong asymptotic behavior in the range of $r > 2$. In Fig. 3, where we employed the large basis sets for both the orbitals and potential, we accomplish perfect agreement between the exchange potential of the LCAO OEP method and the correct potential in the range of $0 < r < 4$. Although it is not evident from the figure, the exchange potential of the LCAO OEP method starts to deviate from the correct potential at around $r = 4$ as the former potential decays rapidly and stays at a

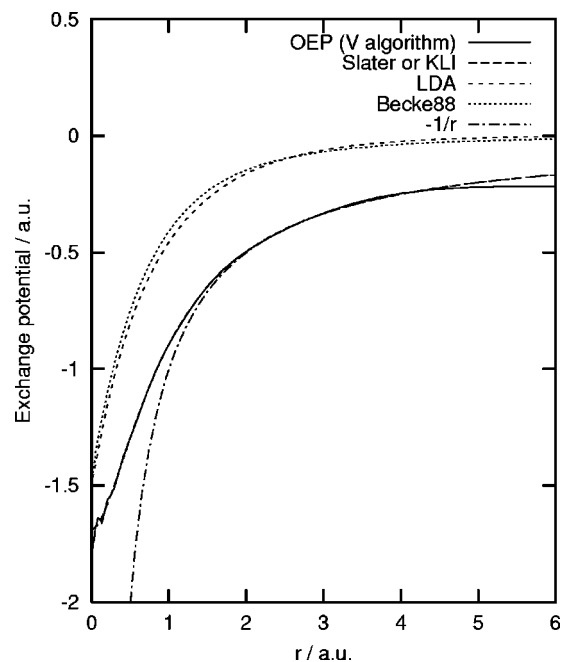


FIG. 4. The exchange potentials of the helium atom as a function of the distance from the nucleus (r). We employ the small basis set for the orbitals and the large basis set for the potential (see the caption of Fig. 1). The exchange potential obtained from the V algorithm of the LCAO OEP method is shifted by -0.2198 a.u.

constant value (which is equal to the value of the shift given to the potential) at large r , while the latter potential decays slowly as $-1/r$. This is inevitable because in the S algorithm the potential is expanded as a linear combination of Gaussian functions and it exhibits the Gaussian decay.

In Figs. 4–6, we repeat the calculations for the helium atom using the small, medium, and large orbital basis sets, respectively, with the V algorithm. We observe qualitatively the same trend that we have observed in Figs. 1–3, but in a much less dramatic way. As we increase the size of the orbital basis set from small to medium, medium to large, the quality of the exchange potential of the LCAO OEP method improves systematically. For instance, in Fig. 4, an unphysical wiggle of the potential is visible at around the nucleus and the potential starts to deviate from the correct $-1/r$ asymptotic behavior at around $r = 3$. In Fig. 5, the wiggle at the nucleus is suppressed significantly, and the potential follows the $-1/r$ behavior until r reaches 4.5 . In Fig. 6, we again obtain excellent agreement between the exchange potential of the LCAO OEP method and the correct potential. Although the potential is expressed as a Coulomb potential created by a charge in the V algorithm and hence it can potentially have the correct $-1/r$ behavior throughout the space, it does not generally do so in the regions where r is large. As a consequence, to obtain a perfect fit between the calculated and analytical solution of the OEP equation, we need to add a significantly large constant (-0.15 a.u.) to the former potential. It must not be misinterpreted, however, that the origin of this seemingly constant displacement is the singularity of $X_{\sigma}(\mathbf{r}_1, \mathbf{r}_2)$ in the infinite basis set limit. This displacement arises primarily from computational effects, more specifically, from the fact that the potential at large r is not

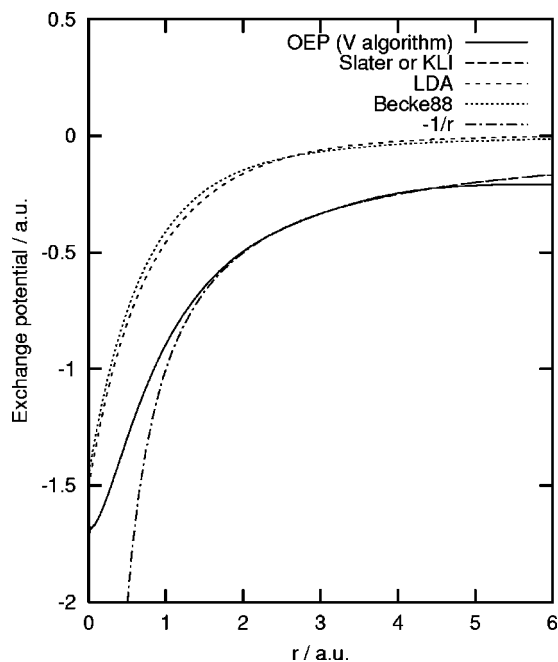


FIG. 5. The exchange potentials of the helium atom as a function of the distance from the nucleus (r). We employ the medium basis set for the orbitals and the large basis set for the potential (see the captions of Figs. 1 and 2). The exchange potential obtained from the V algorithm of the LCAO OEP method is shifted by -0.2131 a.u.

sampled when the exchange matrix elements are evaluated because of the vanishingly small amplitudes of all the orbitals, and hence it tends to have a distorted shape at large r to achieve the minimal total energy (*vide post*). Note that the V algorithm guarantees that the potential decays in inverse pro-

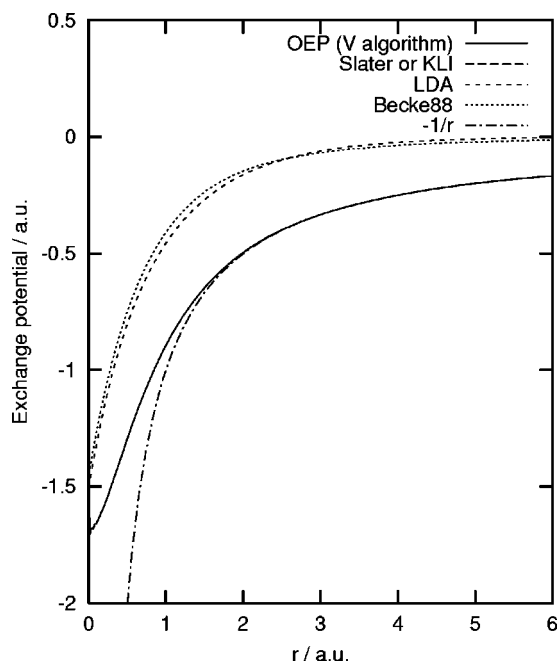


FIG. 6. The exchange potentials of the helium atom as a function of the distance from the nucleus (r). We employ the large basis set for the orbitals and the potential (see the caption of Fig. 1). The exchange potential obtained from the V algorithm of the LCAO OEP method is shifted by -0.1533 a.u. The OEP potential and the Slater or KLI potential are hardly discernible.

portion to r in the asymptotic region, but the prefactor may differ from -1 . It may also be noticed that the deviation from the exchange virial theorem or Eq. (21) (Table I) reflects the quality of the calculated exchange potentials across the S and V algorithms and it decreases systematically with increasing the size of the orbital basis set.^{33,36,37}

We summarize the numerical problems that we encountered in the calculations of the helium atom potential as follows. (1) The exchange potentials obtained from both the S and V algorithms do not have the correct $-1/r$ behavior. As r becomes larger, the potentials tend to distort from the correct shape. (2) The exchange potentials obtained from both the S and V algorithms tend to have the unphysical rapid oscillation around the nucleus. (3) The potentials, and hence the orbital energies also (Table I), are substantially displaced from the correct potentials and orbital energies. When we apply a constant shift to the potential so that the HOMO condition is satisfied, the potential also matches the correct potential in the intermediate range of r . (4) The use of larger and larger orbital basis sets tends to alleviate the above-mentioned problems systematically. In contrast, the use of larger and larger basis sets for the potential itself does not normally alleviate the situation, but can often aggravate the problem. (5) The total energy (and in this two-electron case, the occupied orbital as well) is hardly affected by the shape of the potential or the size of the orbital basis set (Table I). This is true even when the potential looks disastrously unrealistic as in Fig. 1.

As we have shown in the preceding section, mathematically the OEP equation alone can uniquely specify the exchange potential, with the only indeterminacy being an additive constant. This means that in the limit of an infinitely large orbital basis set, the LCAO OEP method should provide the true solution of the OEP equation for the exchange potential. Thus, we can ascribe the above-mentioned numerical problems in the calculated exchange potentials primarily to the incompleteness of the orbital basis set, although, as we shall discuss in the following, there are also other computational effects involved. This explains the observation (4) that the use of larger orbital basis sets renders the calculated exchange potential to resemble the correct potential more closely. It is the size of the orbital basis sets, but not the size of the potential basis sets, that plays an essential role in obtaining reliable potentials, because the larger the orbital basis set, the more complete the products of all the occupied and virtual orbitals, and the more closely the projected exchange potential $\tilde{V}_{X\sigma}^{\text{OEP}}(\mathbf{r})$ as defined by Eq. (23) or (32) resembles the true solution $V_{X\sigma}^{\text{OEP}}(\mathbf{r})$. In contrast, the requirement for the size of the potential basis set appears to be rather modest, as it is much easier to expand the potentials than the orbitals, the latter being much more complex than the former. Indeed, we find that by using a slightly smaller basis set for potentials than for orbitals, we obtain rather well-balanced results; particularly the unphysical rapid oscillation around the nucleus can be suppressed by using smaller potential basis sets that do not contain very tight Gaussian functions (i.e., Gaussian functions with large exponents). For the same reason, the V algorithm suffers much less from the rapid oscillation around the nucleus; the potential basis func-

tions in the V algorithm are the Coulomb potentials created by Gaussian functions and are more diffuse and slowly varying than the Gaussian functions themselves, and they are not necessarily capable of representing the rapid oscillations. Thus, from a practical viewpoint, it is recommended to use as large a basis set as possible for the orbital basis set and a slightly smaller basis set for the potential basis set.

For a spherical system such as the helium atom, the incompleteness of the orbital basis set has two major sources: the lack of very tight functions that have nonvanishing amplitudes only around the nucleus and of very diffuse functions that have large spatial spread. We consider that the lack of tight functions is the primary cause of the unphysical rapid oscillation around the nucleus. Therefore, we expect that adding more and more tight Gaussian functions to the orbital basis set would alleviate this problem, and the results shown in Figs. 1–6 support this view; as we increase the orbital basis set size, the unphysical oscillation around the nucleus becomes less prominent. The lack of diffuse functions in the orbital basis set may partly be responsible for the distortion of the potential at large r . However, this problem occurs primarily because all the occupied orbitals decay and their amplitudes become computationally zero at large r . The exchange potential can have any arbitrary shape in the region where all the occupied orbitals vanish computationally, without deteriorating the total energy or occupied orbitals, because the potential is not sampled at large r when the exchange matrix elements are evaluated. Thus, the LCAO OEP method tends to optimize the exchange potential so that the total energy is minimal, but at the sacrifice of distorting the potential in the asymptotic region as such a distortion has no effect on the total energy or the occupied orbitals. One option to rectify this problem was proposed by Görling,²⁹ who imposed the condition upon the V algorithm that the exchange potential was created by a charge distribution that integrated to -1 . This condition guarantees that the potentials observe the correct $-1/r$ asymptotic behavior, but the total energy and occupied orbitals may not be optimal. We do not use this additional condition because we prefer to obtain accurate exchange potentials in the region where the occupied orbitals have nonvanishing amplitudes and to achieve the minimal total energies at the sacrifice of the correct asymptotic behavior, which may be recovered by grafting the $-1/r$ curve to the exchange potential.⁶³ Ivanov *et al.*⁶⁴ also proposed a scheme in which the HOMO condition was imposed upon either the S or V algorithm in each SCF cycle with the aid of the Lagrange multiplier method. However, in this study, we do not consider this option, either, for the same reason mentioned above.

When the orbital basis sets are sufficiently large, an exchange potential calculated from the LCAO OEP method agrees reasonably well with the correct potential for the intermediate values of r when the former potential is shifted by an appropriate constant. Likewise, the differences between the orbital energies computed by the LCAO OEP method and the correct values are usually (but not always) approximated well by the same constant (Table I). This additive constant arises primarily from the fact that generally neither the S or V algorithm observes the correct $-1/r$ behavior at large r ,

while they can reproduce the shape of the potentials reasonably accurately for the intermediate values of r . When the S algorithm is employed, the exchange potentials are too shallow as compared with the correct potentials in the whole range of r , owing to the rapid Gaussian falloff of the former potentials. Thus, the exchange potentials obtained from the S algorithm are normally displaced upwards from the correct potentials. The magnitude of the displacement decreases systematically as the orbital basis set increases, but it is not generally possible to achieve the limit in which the displacement vanishes. The exchange potentials obtained from the V algorithm, on the other hand, may be displaced either upwards or downwards from the correct potentials and it is sometimes possible to achieve the limit in which the displacement practically vanishes. It should be emphasized that the origin of this artifactual displacement, which is approximated well by a constant, is not the formal indeterminacy of the exchange potentials of the OEP equation established in the preceding section. Indeed, the difference between the calculated and correct exchange potentials is not strictly a constant but a function which is flat in the intermediate region of r but decays to zero at large r and is one of the null-space functions of the kernel matrix. The exchange potential and the orbitals must satisfy not only Eqs. (1) and (29) but also the self-consistency condition (5) simultaneously. The exchange potential that differs from the true solution of the OEP equation by such a null-space function obviously satisfies the self-consistency condition for the same set of orbitals.

Equations (29) and (49) further indicate a primary difference between the LCAO OEP method and other LCAO SCF methods such as the HF method and various approximate DFT methods. In the latter SCF procedures, the potentials that are needed to define the Fock or KS Hamiltonian matrix elements are given unambiguously in terms of some known quantities (orbitals, density, etc.) in each cycle of SCF. In the LCAO OEP method, on the other hand, only the projection of the $V_{X\sigma}^{\text{OEP}}(\mathbf{r})$ onto the space spanned by $\{\psi_{i\sigma}(\mathbf{r})\psi_{a\sigma}(\mathbf{r})\}$ is unambiguously given in terms of orbitals and orbital energies, but the projection of $V_{X\sigma}^{\text{OEP}}(\mathbf{r})$ onto the null space is not provided by the OEP equation. Therefore, the exchange matrix elements evaluated with $\tilde{V}_{X\sigma}^{\text{OEP}}(\mathbf{r})$ and those with $V_{X\sigma}^{\text{OEP}}(\mathbf{r})$ may be substantially different when the orbital basis set is small. However, the exchange matrix elements that involve an occupied orbital and a virtual orbital remain the same, i.e.,

$$\begin{aligned} & \int \psi_{i\sigma}(\mathbf{r})V_{X\sigma}^{\text{OEP}}(\mathbf{r})\psi_{a\sigma}(\mathbf{r})d\mathbf{r} \\ &= \int \psi_{i\sigma}(\mathbf{r})\tilde{V}_{X\sigma}^{\text{OEP}}(\mathbf{r})\psi_{a\sigma}(\mathbf{r})d\mathbf{r}, \end{aligned} \quad (61)$$

because any null-space function is orthogonal to all the products of occupied and virtual orbitals. Equation (61) indicates that the null-space function introduced in the exchange potentials may rotate the occupied orbitals among themselves and the virtual orbitals among themselves, but does not mix the occupied and virtual orbitals. As the OEP total energy expression, which is the same as the HF total energy expres-

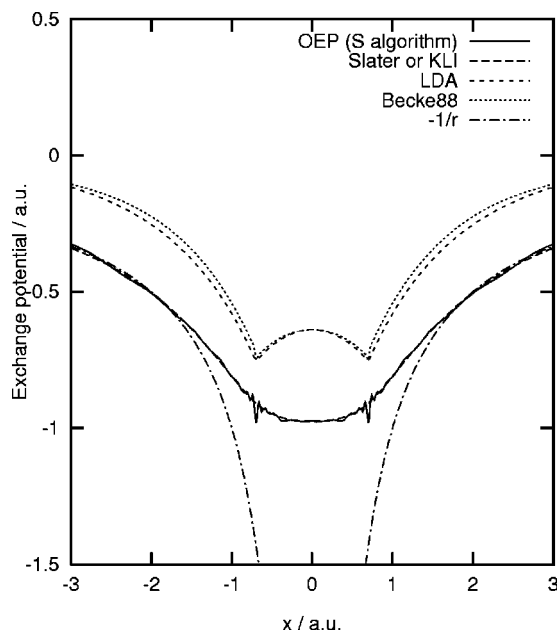


FIG. 7. The exchange potentials of the hydrogen molecule (0.741 \AA) along the C_∞ axis. The orbital basis set and the potential basis set both consist of even-tempered 14 s -type, 5 p -type, and 2 (6-component Cartesian) d -type functions with the exponents given by 0.1×2^n ($0 \leq n \leq 13$), 0.4×4^n ($0 \leq n \leq 4$), and 1.6×4^n ($0 \leq n \leq 1$), respectively. The exchange potential obtained from the S algorithm of the LCAO OEP method is shifted by -0.2664 a.u.

sion, is invariant to the rotation among just the occupied orbitals and the rotation among just the virtual orbitals, the null-space function does not alter the total energy. This explains the above-mentioned observation that even when the exchange potential obtained from the LCAO OEP method is unrealistic as in Fig. 1, the total energy tends to remain accurate and reliable. For the helium atom, where there is only one occupied orbital, the shape of the occupied orbital is also hardly affected by the distortion of the exchange potential, while the orbital energy may be substantially displaced.

As a second example, we choose the hydrogen molecule, for which the Slater and KLI potentials again amount to the correct OEP potential. Figures 7 and 8 are the plot of the exchange potentials computed by the S and V algorithms, respectively, along the C_∞ axis. We find that the exchange potential obtained from the S algorithm has unphysical oscillations around the nuclei but overall it closely approximates the correct potential. These oscillations are suppressed by using the V algorithm (Fig. 8). In the region shown in the figure, the calculated potential also has the correct $-1/r$ behavior, although at large r it starts to deviate from $-1/r$. It may be noticed that the LDA and Becke88 potentials have cusps at the nuclei and are qualitatively different from the correct potential that does not have such cusps. This reflects the fact that the correct potential is an electrostatic potential created by the electron density, Eq. (22), and is a more slowly varying function than the electron density itself. In this light and also remembering that the $-1/r$ asymptotic behavior is essential in the accurate prediction of the positions of Rydberg excited states by time-dependent density functional theory,^{63,65} we consider it an important and interesting problem to develop an exchange functional whose cor-

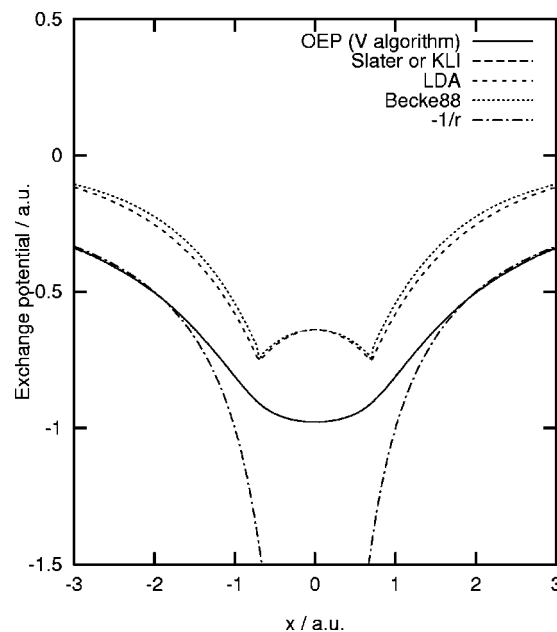


FIG. 8. The exchange potentials of the hydrogen molecule (0.741 \AA) along the C_∞ axis. The basis sets employed are the same as in Fig. 7. The exchange potential obtained from the V algorithm of the LCAO OEP method is shifted by -0.1884 a.u. The OEP potential and the Slater or KLI potential are hardly discernible.

responding exchange potential is an electrostatic potential created by an approximate functional of the electron density.

In Figs. 9 and 10, we plot the exchange potentials of the neon atom computed by the S and V algorithms, respectively, as a function of the distance from the nucleus (r). For this 10-electron system, the Slater potential and the KLI po-

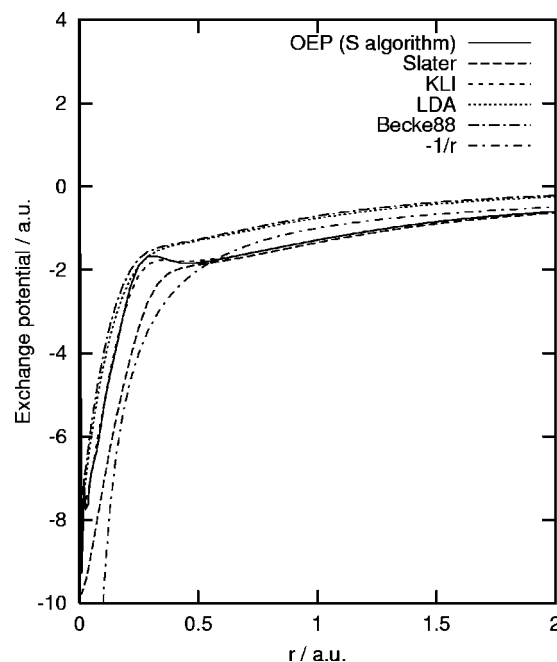


FIG. 9. The exchange potentials of the neon atom as a function of the distance from the nucleus (r). We employ the Partridge-3 basis set for the orbitals and the s -type functions of the same basis set for potential. The exchange potential obtained from the S algorithm of the LCAO OEP method is shifted by -0.2345 a.u.

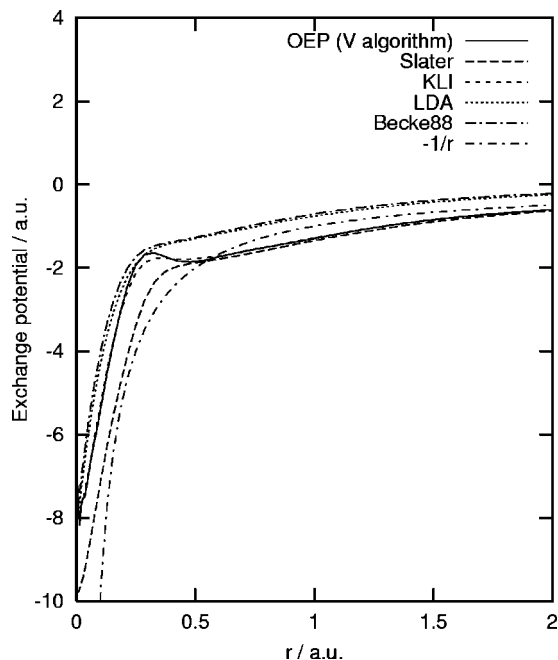


FIG. 10. The exchange potentials of the neon atom as a function of the distance from the nucleus (r). The basis sets employed are the same as in Fig. 9. The exchange potential obtained from the V algorithm of the LCAO OEP method is shifted by -0.0868 a.u.

tential are appreciably different from each other in the vicinity of the nucleus, although they converge at the same $-1/r$ asymptotic curve at large r . The exchange potentials, the total energies, and the orbital energies obtained from the S and V algorithms of the LCAO OEP method are consistent with each other, and hence are reliable except for the unphysical oscillations at the nucleus. They both have the correct $-1/r$ asymptotic behavior in the range of r shown in the figure, and the total energy is also in agreement with the result of the grid-based numerical OEP calculation of Engel and Vosko³⁶ (Table I). The KLI scheme approximates the exchange potential and exchange energy of the LCAO OEP method remarkably well. The only visible difference in the exchange potential is that the structure (bump) at $0.2 < r < 0.6$ in the intershell region is more pronounced in LCAO OEP than in KLI. Note also that the LCAO KLI calculation reproduces the total energy and the highest occupied orbital energy computed by the grid-based numerical KLI calculation⁴⁹ (Table I). The LDA and Becke88 potentials as well as the Slater potential exhibit a marked change in the slope at $r \approx 0.3$, but they do not have the structure in the intershell region, which is known to be important energetically.³³ The LDA and Becke88 predict the potentials that are too shallow almost everywhere in the space as compared with LCAO OEP and KLI, while the Slater potential is too deep in the range of $0 < r < 0.4$, which is documented already.⁸

Figures 11–14 plot the exchange potentials of the nitrogen molecule and lithium fluoride computed by the S and V algorithms along the C_∞ axis of the respective molecules. The requirement for the size of orbital basis set is much greater for these molecules than for spherical systems, and the uncontracted 6-311+ +G(2d,2p) basis set that we em-

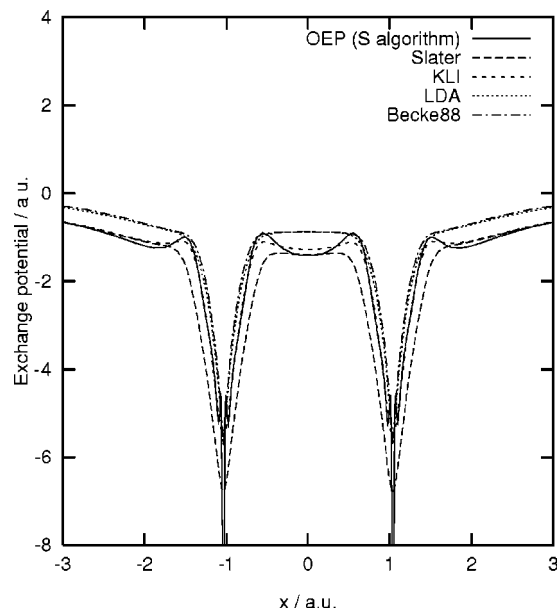


FIG. 11. The exchange potentials of nitrogen molecule (1.098 Å) along the C_∞ axis. We employ an uncontracted 6-311+ +G(2d,2p) basis set for the orbitals and an uncontracted 6-31G basis set supplemented with a set of s -type, p -type, and 6-component Cartesian d -type functions with a shared exponent of 0.8 for the potential. The exchange potential obtained from the S algorithm of the LCAO OEP method is shifted by -0.2523 a.u.

ploy is perhaps among the minimal basis sets for which reasonably reliable exchange potentials can be obtained. For the nitrogen molecule, however, the result of the S algorithm (Fig. 11) slightly differs from that of the V algorithm (Fig. 12) in the depth of the potential at around $x=0$, and accordingly, the deviations from the exchange virial theorem are substantial. For lithium fluoride, we achieve exchange potentials, total energies, and orbital energies that are consistent

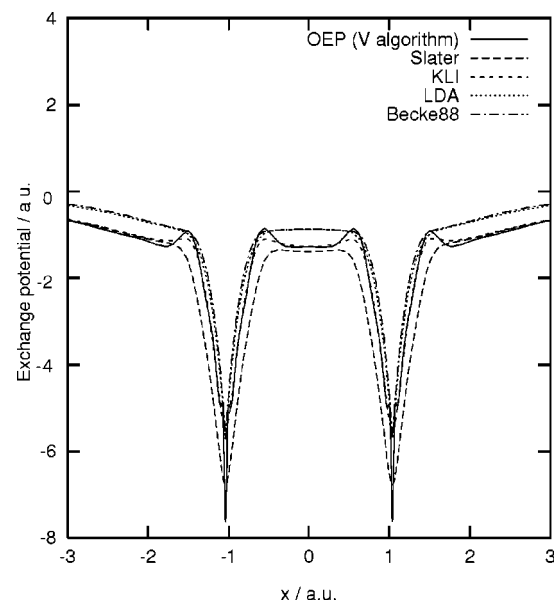


FIG. 12. The exchange potentials of nitrogen molecule (1.098 Å) along the C_∞ axis. The basis sets employed are the same as in Fig. 11. The exchange potential obtained from the V algorithm of the LCAO OEP method is shifted by 0.4362 a.u.

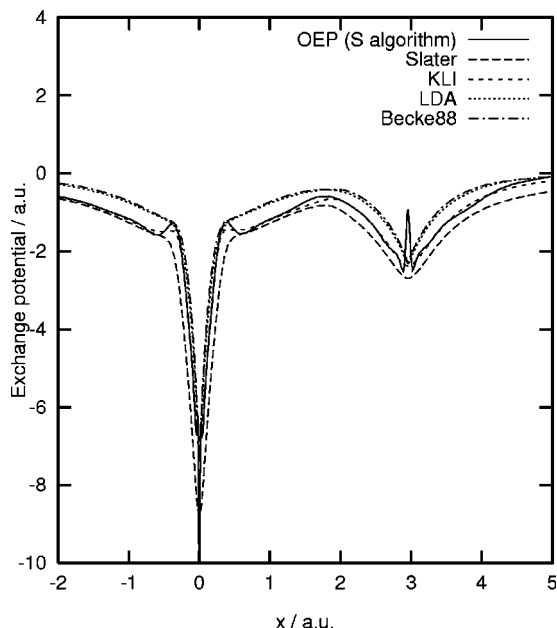


FIG. 13. The exchange potentials of lithium fluoride molecule (1.564 Å) along the C_{∞} axis. We employ an uncontracted 6-311++G(2*d*,2*p*) basis set for the orbitals and an uncontracted 6-31G basis set supplemented with a set of *s*-type, *p*-type, and 6-component Cartesian *d*-type functions with a shared exponent of 0.2 (lithium) and a set of *s*-type, *p*-type, and 6-component Cartesian *d*-type functions with a shared exponent of 0.8 (fluorine) for the potential. The exchange potential obtained from the *S* algorithm of the LCAO OEP method is shifted by -0.0986 a.u.

between the *S* and *V* algorithms, and hence we consider them to be reasonably accurate. In practice, it is difficult to remove the spikes in the exchange potentials of the LCAO OEP method at the nuclei, which are the artifacts arising from the basis-set incompleteness. The KLI potentials again

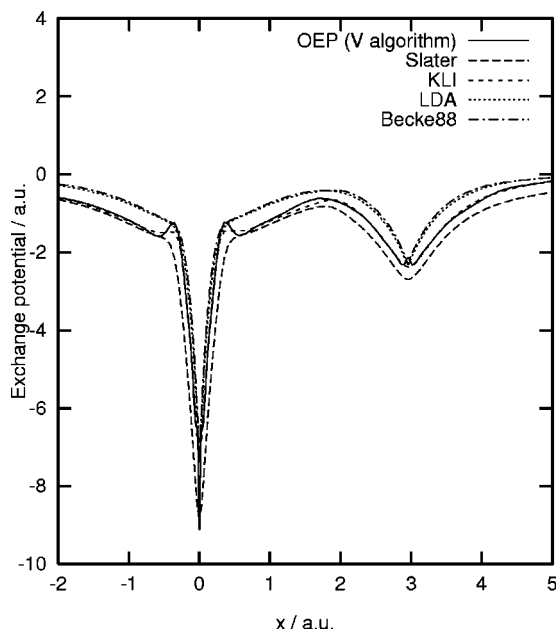


FIG. 14. The exchange potentials of lithium fluoride molecule (1.564 Å) along the C_{∞} axis. The basis sets employed are the same as in Fig. 13. The exchange potential obtained from the *V* algorithm of the LCAO OEP method is shifted by 0.1984 a.u.

approximate the potentials of the LCAO OEP method for both the molecules well. The potentials of the KLI and LCAO OEP methods are indistinguishable from each other in the vicinity of the nuclei and also in the asymptotic region shown in the figures. The KLI potentials have less pronounced structures (bumps) in the intershell regions than the potentials of the LCAO OEP method, and the former appear to smooth the structures of the latter. The comparison of the total energies computed by the LCAO OEP and grid-based numerical KLI methods (Table I) indicates that the basis-set dependence of the total energies is much greater than the errors introduced by the KLI approximation (Ref. 68).

IV. CONCLUSION

We have illustrated the computational difficulties in the LCAO OEP method that we²⁸ and Görling²⁹ have developed recently and identified the source of these difficulties. We have proved that in the limit of an infinite basis set an exchange potential of the OEP method can be uniquely determined up to an additive constant by the OEP equation alone, substantiating the conclusion drawn earlier by Görling and Levy.¹⁸ Therefore, the above-mentioned computational difficulties are primarily due to the incompleteness of the orbital basis set. These effects are more profound on the OEP method than on other SCF procedure such as the LCAO HF or LCAO DFT methods, owing to the fact that the OEP equation unambiguously defines the exchange potential in the space spanned by the product of occupied and virtual orbitals but not in the entire Hilbert space. Nonetheless, by making a judicious choice of the orbital and potential basis sets, we can obtain reasonably accurate exchange potentials for atoms and molecules. Generally, a large uncontracted basis set must be employed for orbitals, whereas for the potential, a basis set that is smaller than the orbital basis set is recommended. Even when the orbital basis set is sufficiently large to accurately reproduce the exchange potential in the vicinity of the nuclei, it is usually difficult to achieve the correct $-1/r$ decay throughout the asymptotic region, as the occupied orbitals vanish computationally at large r . Consequently, we must shift the calculated exchange potentials so that the HOMO condition is satisfied for the shifted potentials. We have observed that, for the systems where the correct exchange potentials are analytically known, this procedure provides us with an exchange potential of the OEP method that is indistinguishable from the correct potential in the vicinity of the nuclei and in a respectable portion of the asymptotic region. For larger atomic and molecular systems, two different algorithms provide exchange potentials that are consistent with each other when sufficiently large orbital basis sets are employed, and hence we consider that they are reasonably converged. Not only for atoms but also for molecules, the KLI approximation has turned out to be accurate and robust, although it misses some structures in the intershell regions, and is a pragmatic means of generating reference exchange potentials against which approximate exchange functionals can be tested and calibrated.^{66–70} However, the OEP method itself, as well as the KLI scheme, will continue to serve as a universal technique for mapping a nonlocal potential onto a local potential and is essential in

obtaining accurate correlation potentials from some explicitly orbital-dependent correlation functionals established in the complementary wave function theory.²⁶

ACKNOWLEDGMENTS

The authors gratefully acknowledge Professor Mel Levy (Tulane University), Professor Robert K. Nesbet (IBM Almaden Research Center), Dr. S. Ajith Perera (University of Florida), and Professor Weitao Yang (Duke University) for illuminating discussions. This work has been supported by the U.S. Air Force Office of Scientific Research under Grant No. F49620-98-0116 and the Natural Sciences and Engineering Research Council of Canada. One of the authors (K.B.) was supported by the National Science Foundation under Grant No. CHE-9875091.

- ¹R. T. Sharp and G. K. Horton, *Phys. Rev.* **90**, 317 (1953).
- ²J. D. Talman and W. F. Shadwick, *Phys. Rev. A* **14**, 36 (1976).
- ³P. Hohenberg and W. Kohn, *Phys. Rev.* **136**, B864 (1964).
- ⁴W. Kohn and L. J. Sham, *Phys. Rev.* **140**, A1133 (1965).
- ⁵R. G. Parr and W. Yang, *Density-Functional Theory of Atoms and Molecules* (Oxford University Press, New York, 1989), and references therein.
- ⁶V. Sahni, J. Gruenebaum, and J. P. Perdew, *Phys. Rev. B* **26**, 4371 (1982).
- ⁷J. P. Perdew and M. R. Norman, *Phys. Rev. B* **26**, 5445 (1982).
- ⁸J. B. Krieger, Y. Li, and G. J. Iafrate, *Phys. Rev. A* **45**, 101 (1992).
- ⁹J. P. Perdew, R. G. Parr, M. Levy, and J. L. Balduz, Jr., *Phys. Rev. Lett.* **49**, 1691 (1982).
- ¹⁰J. P. Perdew and M. Levy, *Phys. Rev. Lett.* **51**, 1884 (1983).
- ¹¹L. J. Sham and M. Schlüter, *Phys. Rev. Lett.* **51**, 1888 (1983).
- ¹²S. K. Ghosh and R. G. Parr, *J. Chem. Phys.* **82**, 3307 (1985).
- ¹³M. Levy and J. P. Perdew, *Phys. Rev. A* **32**, 2010 (1985).
- ¹⁴K. Aashamar, T. M. Luke, and J. D. Talman, *J. Phys. B* **12**, 3455 (1979).
- ¹⁵K. Aashamar, T. M. Luke, and J. D. Talman, *J. Phys. B* **14**, 803 (1981).
- ¹⁶N. E. Zein, *J. Phys. C* **17**, 2107 (1984).
- ¹⁷L. J. Sham, *Phys. Rev. B* **32**, 3876 (1985).
- ¹⁸A. Görling and M. Levy, *Phys. Rev. A* **50**, 196 (1994).
- ¹⁹A. Görling and M. Levy, *Int. J. Quantum Chem., Symp.* **29**, 93 (1995).
- ²⁰M. E. Casida, *Phys. Rev. A* **51**, 2005 (1995).
- ²¹M. E. Casida, *Phys. Rev. B* **59**, 4694 (1999).
- ²²S. Ivanov, K. Burke, and M. Levy, *J. Chem. Phys.* **110**, 10262 (1999).
- ²³E. Engel and R. M. Dreizler, *J. Comput. Chem.* **20**, 31 (1999).
- ²⁴T. Grabo, T. Kreibich, S. Kurth, and E. K. U. Gross, *Orbital functionals in density functional theory: the optimized effective potential method, in Strong Coulomb Correlations and Electronic Structure Calculations*, edited by V. I. Anisimov (Gordon and Breach, London, 1999).
- ²⁵S. Ivanov and R. J. Bartlett, *J. Chem. Phys.* **114**, 1952 (2001).
- ²⁶I. Grabowski *et al.* (unpublished).
- ²⁷R. J. Bartlett, *Quantum Chemistry in the New Millennium: The Next Step, in Chemistry for the 21st Century*, edited by E. Keinan and I. Schechter (Wiley-VCH, Weinheim, 2000).
- ²⁸S. Ivanov, S. Hirata, and R. J. Bartlett, *Phys. Rev. Lett.* **83**, 5455 (1999).
- ²⁹A. Görling, *Phys. Rev. Lett.* **83**, 5459 (1999).
- ³⁰K. Aashamar, T. M. Luke, and J. D. Talman, *At. Data Nucl. Data Tables* **22**, 443 (1978).
- ³¹M. R. Norman and D. D. Koelling, *Phys. Rev. B* **30**, 5530 (1984).
- ³²J. D. Talman, *Comput. Phys. Commun.* **54**, 85 (1989).
- ³³Y. Wang, J. P. Perdew, J. A. Chevary, L. D. Macdonald, and S. H. Vosko, *Phys. Rev. A* **41**, 78 (1990).
- ³⁴J. B. Krieger, Y. Li, and G. J. Iafrate, *Phys. Lett. A* **146**, 256 (1990).
- ³⁵J. B. Krieger, Y. Li, and G. J. Iafrate, *Phys. Rev. A* **46**, 5453 (1992).
- ³⁶E. Engel and S. H. Vosko, *Phys. Rev. A* **47**, 2800 (1993).
- ³⁷E. Engel and S. H. Vosko, *Phys. Rev. B* **47**, 13164 (1993).
- ³⁸R. K. Nesbet and R. Colle, *Phys. Rev. A* **61**, 012503 (1999).
- ³⁹R. K. Nesbet and R. Colle, *J. Math. Chem.* **26**, 233 (1999).
- ⁴⁰R. Colle and R. K. Nesbet (unpublished).
- ⁴¹D. C. Langreth and M. J. Mehl, *Phys. Rev. B* **28**, 1809 (1983).
- ⁴²T. Kotani, *Phys. Rev. B* **50**, 14816 (1994); **51**, 13903(E) (1995).
- ⁴³T. Kotani, *Phys. Rev. Lett.* **74**, 2989 (1995).
- ⁴⁴T. Kotani and H. Akai, *Phys. Rev. B* **54**, 16502 (1996).
- ⁴⁵M. Städele, J. A. Majewski, P. Vogl, and A. Görling, *Phys. Rev. Lett.* **79**, 2089 (1997).
- ⁴⁶M. Städele, M. Moukara, J. A. Majewski, P. Vogl, and A. Görling, *Phys. Rev. B* **59**, 10031 (1999).
- ⁴⁷J. C. Slater, *Phys. Rev.* **81**, 385 (1951).
- ⁴⁸Y. Li, J. B. Krieger, M. R. Norman, and G. J. Iafrate, *Phys. Rev. B* **44**, 10437 (1991).
- ⁴⁹Y. Li, J. B. Krieger, and G. J. Iafrate, *Phys. Rev. A* **47**, 165 (1993).
- ⁵⁰R. P. Kanwal, *Linear Integral Equations: Theory and Technique*, 2nd ed. (Birkhäuser, Boston, 1997).
- ⁵¹L. M. Delves and J. L. Mohamed, *Computational Methods for Integral Equations* (Cambridge University Press, Cambridge, 1985).
- ⁵²S. Hirata, M. Tasumi, H. Torii, S. Iwata, M. Head-Gordon, and R. J. Bartlett, *POLYMER* Version 1.0, 1999.
- ⁵³S. Obara and A. Saika, *J. Chem. Phys.* **84**, 3963 (1986).
- ⁵⁴J. Andzelm and E. Wimmer, *J. Chem. Phys.* **96**, 1280 (1992).
- ⁵⁵V. Termath and N. C. Handy, *Chem. Phys. Lett.* **230**, 17 (1994).
- ⁵⁶A. D. Becke, *J. Chem. Phys.* **88**, 2547 (1988).
- ⁵⁷S. Hirata, H. Torii, and M. Tasumi, *Phys. Rev. B* **57**, 11994 (1998).
- ⁵⁸V. I. Lebedev, *Zh. Vychisl. Mat. Mat. Fiz.* **15**, 48 (1975).
- ⁵⁹V. I. Lebedev, *Zh. Vychisl. Mat. Mat. Fiz.* **16**, 293 (1976).
- ⁶⁰V. I. Lebedev, *Sibirsk. Mat. Zh.* **18**, 132 (1977).
- ⁶¹J. C. Slater, *Quantum Theory of Molecules and Solids, Vol. 4: The Self-Consistent Field for Molecules and Solids* (McGraw-Hill, New York, 1974).
- ⁶²A. D. Becke, *Phys. Rev. A* **38**, 3098 (1988).
- ⁶³D. J. Tozer and N. C. Handy, *J. Chem. Phys.* **109**, 10180 (1998).
- ⁶⁴S. Ivanov *et al.* (unpublished).
- ⁶⁵M. E. Casida, C. Jamorski, K. C. Casida, and D. R. Salahub, *J. Chem. Phys.* **108**, 4439 (1998).
- ⁶⁶T. Grabo and E. K. U. Gross, *Chem. Phys. Lett.* **240**, 141 (1995).
- ⁶⁷T. Grabo and E. K. U. Gross, *Int. J. Quantum Chem.* **64**, 95 (1997).
- ⁶⁸E. Engel, A. Höck, and R. M. Dreizler, *Phys. Rev. A* **62**, 042502 (2000).
- ⁶⁹P. Süle, S. Kurth, and V. Van Doren, *J. Chem. Phys.* **112**, 7355 (2000).
- ⁷⁰J. Garza, J. A. Nichols, and D. A. Dixon, *J. Chem. Phys.* **112**, 7880 (2000).